

# NASA CONTRACTOR REPORT



NASA CR-1751

0060728

TECH LIBRARY KAFB, NM

NASA CR-1751

LOAN COPY: RETURN TO  
AFWL (DOGL)  
KIRTLAND AFB, N. M.

## EXPERIMENTAL ATMOSPHERIC ABSORPTION VALUES FROM AIRCRAFT FLYOVER NOISE SIGNALS

*by*

*Dwight E. Bishop and Myles A. Simpson  
Bolt Beranek and Newman, Inc.*

*and*

*David Chang  
Allied Research Associates, Inc.*

*Prepared by*

**BOLT BERANEK AND NEWMAN, INC.**

Van Nuys, Calif. 91406

*for Langley Research Center*



0060728

1. Report No. NASA CR-1751		2. Government Accession No.		3. Recipient's Catalog No.	
4. Title and Subtitle  EXPERIMENTAL ATMOSPHERIC ABSORPTION VALUES FROM AIRCRAFT FLYOVER NOISE SIGNALS				5. Report Date June 1971	
				6. Performing Organization Code	
7. Author(s) Dwight E. Bishop and Myles A. Simpson--Bolt Beranek and Newman, Inc. David Chang--Allied Research Associates, Inc.				8. Performing Organization Report No. 1868	
9. Performing Organization Name and Address Bolt Beranek and Newman, Inc. 15808 Wyandotte Street Van Nuys, California 91406				10. Work Unit No. 126-61-14-01	
				11. Contract or Grant No. NASI - 8168	
12. Sponsoring Agency Name and Address NASA - Langley Research Center Hampton, Virginia 23365				13. Type of Report and Period Covered Contractor Report	
				14. Sponsoring Agency Code	
15. Supplementary Notes					
16. Abstract  A detailed analysis of the noise recorded on the ground during a series of 20 aircraft flyovers by two aircraft (a four-engine turbojet transport and a four-engine piston transport) during a single day of field measurements has been conducted to obtain experimental values of sound absorption. Noise levels recorded at five positions under and to the side of the flight path together with radar tracking data and meteorological information obtained on the surface and aloft were acquired during the field tests. Differences in one-third octave band noise levels observed at different ground positions for the same angle of radiation from the aircraft were utilized to obtain sets of absorption values which are compared to calculated values of sound absorption using both surface and altitude measurements of temperature and humidity.					
17. Key Words (Suggested by Author(s))  Aircraft Flyover Noise Atmospheric Noise Absorption				18. Distribution Statement  Unclassified - Unrestricted	
19. Security Classif. (of this report) Unclassified		20. Security Classif. (of this page) Unclassified		21. No. of Pages 72	
				22. Price* \$3.00	



## TABLE OF CONTENTS

	<u>Page</u>
SUMMARY . . . . .	1
INTRODUCTION . . . . .	3
BACKGROUND DISCUSSION . . . . .	4
MEASUREMENT PROGRAM . . . . .	10
Description of Field Measurements . . . . .	10
Meteorological Measurements . . . . .	11
MEASUREMENT RESULTS . . . . .	16
Calculated Atmospheric Absorption . . . . .	16
Measured Atmospheric Absorption Values. . . . .	17
Measurement Variability. . . . .	22
Signal-to-Noise Limitations at High Frequencies. . . . .	25
CONCLUSIONS. . . . .	27
REFERENCES . . . . .	31
TABLES . . . . .	32
FIGURES . . . . .	37
APPENDIX A . . . . .	A-1
APPENDIX B . . . . .	B-1

## LIST OF TABLES

- Table I - LOG OF AIRCRAFT TEST FLIGHTS - 29 APRIL 1969,  
NASA, WALLOPS STATION, VIRGINIA
- Table II - TYPICAL SURFACE WEATHER PARAMETERS DURING  
FLIGHTS
- Table III - AVERAGE ATMOSPHERIC ABSORPTION VALUES BASED  
UPON SAE ARP 866 CALCULATIONS
- Table IV - AVERAGE EXPERIMENTAL ATMOSPHERIC ABSORPTION  
VALUES FOR FLIGHTS ON APRIL 29, 1969\*
- Table V - TYPICAL STANDARD DEVIATION FOR SOUND LEVELS\*  
MEASURED DURING REPEAT FLYOVERS OF FOUR-ENGINE  
TURBOJET AIRPLANE AT NOMINAL 2000 FT ALTITUDE
- Table VI - COMPARISON OF ACOUSTIC AND DATA ACQUISITION  
REDUCTION SYSTEM BACKGROUND NOISE FLOORS

## LIST OF FIGURES

- Figure 1 - SKETCH OF IDEALIZED MEASUREMENT ARRANGEMENT FOR STUDY OF AIR-TO-GROUND SOUND PROPAGATION
- Figure 2 - SKETCH OF MEASUREMENT SETUP SHOWING LIMITING ELEVATION ANGLES
- Figure 3 - LOCATIONS OF NOISE MEASUREMENT POSITIONS WITH RESPECT TO AIRCRAFT PATH
- Figure 4 - TYPICAL FLYOVER NOISE MEASUREMENT INSTRUMENTATION
- Figure 5 - TEMPERATURE VARIATIONS DURING AFTERNOON FLYOVER MEASUREMENTS
- Figure 6 - ABSOLUTE HUMIDITY VARIATION DURING AFTERNOON FLYOVER MEASUREMENTS
- Figure 7 - APPROXIMATE TEMPERATURE AND ABSOLUTE HUMIDITY PROFILES DURING MORNING FLYOVER MEASUREMENTS
- Figure 8 - SCHEMATIC OF DATA ANALYSIS
- Figure 9 - ATMOSPHERIC ABSORPTION VALUES FOR SURFACE AND ALTITUDE MEASUREMENTS OF TEMPERATURE AND HUMIDITY, CALCULATED IN ACCORDANCE WITH SAE ARP 866
- Figure 10 - EXCESS ATTENUATION VERSUS INCREMENTAL PROPAGATION DISTANCE - Convair 880 Flyover, 1500 ft Altitude, Afternoon Run (Event 211) - 1000 Hz
- Figure 11 - EXCESS ATTENUATION VERSUS INCREMENTAL PROPAGATION DISTANCE - Convair 880 Flyover, 1500 ft Altitude, Afternoon Run (Event 211) - 4000 Hz
- Figure 12 - COMPARISON OF AVERAGE ABSORPTION CURVES FROM DIFFERENT TYPES OF REGRESSION LINES - Afternoon Runs of the Convair 880

## LIST OF FIGURES (Con't)

- Figure 13 - VARIATION OF ATMOSPHERIC ABSORPTION WITH  
FREQUENCY - Morning Runs of the Convair 880
- Figure 14 - VARIATION OF ATMOSPHERIC ABSORPTION WITH  
FREQUENCY - Afternoon Runs of the Convair 880
- Figure 15 - VARIATION OF ATMOSPHERIC ABSORPTION WITH  
FREQUENCY - Afternoon Runs of the Lockheed 1049G
- Figure 16 - COMPARISON OF AVERAGE ATMOSPHERIC ABSORPTION  
CURVES - (Extrapolated Tracking Data Included)
- Figure 17 - COMPARISON OF AVERAGE ATMOSPHERIC ABSORPTION  
CURVES - (Extrapolated Tracking Data Removed)
- Figure 18 - COMPARISONS OF AVERAGE ATMOSPHERIC ABSORPTION  
CURVES FOR FLIGHTS AT 1500 FT ALTITUDE -  
(Extrapolated Tracking Data Removed)
- Figure 19 - COMPARISON OF AVERAGE EXPERIMENTAL VALUES OF  
ATMOSPHERIC ABSORPTION WITH SAE 866 CALCULATED  
VALUES
- Figure 20 - AVERAGE ATMOSPHERIC ABSORPTION CURVES FOR  
DIFFERENT RADIATION ANGLES - LOCKHEED 1049G  
(Extrapolated Tracking Data Removed)
- Figure 21 - AVERAGE ATMOSPHERIC ABSORPTION CURVES FOR  
DIFFERENT RADIATION ANGLES - Convair 880  
(Extrapolated Tracking Data Removed)
- Figure 22 - STANDARD DEVIATION FOR SEVEN REPEAT MEASUREMENTS  
OF ONE-THIRD OCTAVE BAND SOUND LEVELS DURING  
TURBOJET TRANSPORT AIRCRAFT FLYOVERS AT 2000 FT  
ALTITUDE - (Position 2, Beneath Flight Path)

EXPERIMENTAL ATMOSPHERIC ABSORPTION VALUES FROM  
AIRCRAFT FLYOVER NOISE SIGNALS

By Dwight E. Bishop and Myles A. Simpson  
Bolt Beranek and Newman, Inc.

David Chang  
Allied Research Associates, Inc.

SUMMARY

A detailed analysis of the noise recorded on the ground during a series of 20 aircraft flyovers by two aircraft (a four-engine turbojet transport and a four-engine piston transport) during a single day of field measurements has been conducted to obtain experimental values of sound absorption. Noise levels recorded at five positions under and to the side of the flight path together with radar tracking data and meteorological information obtained on the surface and aloft were acquired during the field tests. Differences in one-third octave band noise levels observed at different ground positions for the same angle of radiation from the aircraft were utilized to obtain sets of absorption values which are compared to calculated values of sound absorption using both surface and altitude measurements of temperature and humidity.

During the tests, moderate surface temperatures (58 to 61° F.) and high relative humidities (80 to 100%) were experienced. For these particular tests, little difference was found between mean calculated absorption values based upon surface measurements alone compared to those calculated from both surface and altitude measurements of temperature and humidity.



Although considerable variability was found among absorption values calculated from single flyovers, confidence level intervals were considerably reduced by grouping data from several flyovers. Mean experimental atmospheric absorption values based upon combined data for all flyovers show good agreement (within  $\pm 0.8$  dB per 1000 ft) with calculated absorption values for frequencies from 1250 to 6300 Hz. At frequencies from 400 Hz (the lower frequency limit of the study) to 1000 Hz, the experimental values, typically 2 dB per thousand feet, are significantly greater than calculated values based upon the existing industry guide, SAE ARP 866. At 8000 Hz, experimental data show considerable scatter and conflicting results with calculated values.

The experimental values of atmospheric absorption are consistently lower for large radiation angles (110 to 150° as measured from the forward direction of the aircraft) from the turbojet aircraft compared to the values for other radiation angles from the turbojet aircraft or for all radiation angles from the propeller aircraft.

The data analysis techniques and field procedures appear useful for application in additional studies of sound absorption over a wider range of temperature and humidity. Recommendations for changes in instrumentation are given in order to obtain more useful data in the frequency range from 6300 to 10,000 Hz.

## INTRODUCTION

This report describes the results of analyses of sets of recorded flyover noise data to obtain experimental values of atmospheric absorption coefficients. The test data were obtained on April 29, 1969 during a single day of field measurements in which a series of 20 controlled aircraft flyovers were made -- 14 flyovers of a four-engine turbojet transport aircraft (Convair 880), and 6 flyovers of a four-engine piston power aircraft (Lockheed 1049G). The major purposes of the program were to:

- a) Develop and test methods for analyzing flyover signals received at different ground positions to obtain experimental values of air absorption.
- b) Compare the experimental values of sound absorption with those predicted by available industry guides using both surface and altitude values of temperature and humidity.
- c) On the basis of the above, develop conclusions and recommendations for future sound propagation studies.

## BACKGROUND DISCUSSION

The noise signals received on the ground from noise propagated from an aircraft during a flyover are subject to many influences as the signal propagates through the atmosphere. Temperature and wind gradients produce differences in sound speeds in different portions of the atmosphere which result in "bending" of the sound propagation paths. Inhomogeneities in the atmosphere cause scattering; the terrain introduces absorption and reflections. In addition to such factors, sound is attenuated as it travels through the atmosphere primarily as a result of molecular absorption. Such absorption by the atmosphere varies with both the temperature and humidity of the air.

Because atmospheric conditions are seldom the same, there is need for methods for comparing flyover noise levels obtained under one set of field conditions with those observed under different atmospheric conditions, or, to adjust experimentally obtained flyover noise levels to those which would be expected for "standard" atmospheric conditions. SAE Aerospace Recommended Practice (ARP) 866 (Ref. 1) presents a method for estimating the atmospheric absorption of sound due to both classical and molecular attenuation for a wide range of temperatures, humidities and frequencies.

Field atmospheric absorption data obtained from aircraft flyovers reported from a variety of sources show conflicting agreement with ARP 866 values. Some of the experimental data shows good agreement with ARP 866 values but much of the reported data often falls below and sometimes above the predicted values at the higher frequencies (Refs. 2, 3 and 4).

A possible important contributor to the scatter in experimental data is the fact that, for most reported data, only surface measures of temperature and humidity were made and little information is available to indicate whether or not absorption may have varied at heights between the surface and the aircraft.

The scatter in experimental data has stimulated interest in means for improving atmospheric absorption prediction procedures and/or refining test procedures to obtain more reliable field data. One approach is to specify more rigorously the meteorological conditions under which flight measurements should be made. For example, the weather conditions outlined for noise certification requirements (Ref. 5) specify ranges of surface winds, temperature and humidity under which acceptable measurements may be made. A drawback to this approach is that it drastically limits the time and places under which acceptable noise measurements may be made. Further, there is at present no certainty, substantiated by experimental evidence, that the specified meteorological conditions satisfactorily remove the uncertainty about atmospheric absorption corrections.

Another factor contributing to the scatter of data at the higher audio frequencies is the difficulty in obtaining reliable noise measurements at the higher frequencies, particularly above 4000 Hz, due to basic signal-to-noise limitations. Such limitations result from the generally decreasing noise output of most aircraft sources at the higher frequencies and the large increases in atmospheric absorption with frequency. Both factors contribute to a sharp decrease in the received flyover noise signal as a function of frequency. Further factors contributing to scatter at higher frequencies are uncertainties in microphone frequency response due to variations in microphone response with changing angles of incidence.

A major limitation entering into the determination of excess absorption values from flyover noise signals (typically produced by aircraft flying at speeds from

150 to 250 knots at altitudes from 500 to 2000 ft) is the time-varying nature of the signal received on the ground, which drastically limits the time over which the signal level can be meaningfully averaged. Although the basic noise signal produced by the aircraft is usually broad band in nature and may resemble random noise when measured in the near field, the signal received at a large distance from the source will undergo fluctuations, as measured in  $1/3$  octave bands, that are of much greater variability than would be expected for a random noise signal. Thus, given a limited sampling time, and the unknown but suspected large variation in signal amplitude, data from a single flyover measurement must be associated with a relatively large confidence interval about it.

The field measurement program was devised to eliminate or reduce some of the limitations frequently encountered in past measurements. In particular, temperature, humidity and winds were measured at the surface and aloft. Special low-frequency de-emphasis networks were incorporated in the noise recording system to improve the signal-to-noise ratio of the recorded signal at the higher audio frequencies. The basic sample time limitation was approached by utilizing, typically, twenty-five measurements of levels at different time intervals per flyover record for each one-third octave frequency band at each ground position, and recording the flyover at five ground positions. Also, flyovers of an aircraft at the same altitude were repeated for each series of flyover tests.

Before reviewing details of the field experiment, it is helpful to first outline the basic approach used in correlating the aircraft and noise data and in matching noise data obtained at different ground positions and

at different time intervals during a single aircraft flyover. The analysis approach is made practicable by the availability of accurate aircraft tracking information and time correlations between aircraft positions and the noise measurements recorded at ground positions.

The approach utilizes several basic assumptions about the aircraft sound source. Primary assumptions are (a) the aircraft noise output for any one flyover at constant air speed and altitude is constant and does not change during the flyover; (b) the directional pattern of sound radiation from the aircraft is cylindrically symmetric about the aircraft flight path; (c) the size of the aircraft sound source is small compared to the measurement distances involved.

Obviously, assumptions (b) and (c) are not true at small distances from multi-engine aircraft. However, for the distances concerned, ranging from a minimum altitude of approximately 700 ft for the four-engine piston aircraft and 1500 ft for the turbojet aircraft, assumption (b) was assumed to be a reasonable one that would not introduce large errors. Assumption (c) also appeared quite reasonable for the piston aircraft for the measurement distances involved. It may be a more questionable assumption for the jet aircraft where the effective size of the radiating sound source is more difficult to define, and where source size may vary significantly with frequency. However, for the frequency range above 1000 Hz, which is of most interest in the measurements, the assumption does not appear unreasonable.

The approach does not depend upon several assumptions which are often used in comparing flyover noise data to obtain excess sound absorption coefficients. No assumptions are made as to the uniformity of the sound source from flight to flight. And, no assumptions are involved as to the uniformity of sound power output and/or directivity characteristics for flights made at different altitudes.

The analysis concept is illustrated in the simplified sketch of aircraft flight paths and ground measurement positions sketched in Fig. 1. Noise signals from an aircraft flying at constant altitude and heading above the ground are recorded at several ground positions underneath and to either side of the aircraft flight path. Time correlations are maintained so that the signal received at any instant of time at a ground position can be related to the aircraft flight position, after taking into account the average speed of sound. In analysis, portions of flyover signals propagated at the same angle of radiation from the aircraft flight path are compared for two ground positions. Noise levels and propagation distances are determined for both positions for the given angle of radiation.

For example, using the ground positions, A and B, and the angles identified in Fig. 1, when angles  $\theta_A$  and  $\theta_B$  equal an arbitrary angle  $\theta_X$ , the sound levels  $L_A(X)$  and  $L_B(X)$  and propagation distances  $d_A(X)$  and  $d_B(X)$  can be determined.

The experimental value of atmospheric absorption can be determined for the difference in propagation distances. Thus, for the difference in propagation distance, the atmospheric absorption,  $m$ , is:

$$m = L_A(X) - L_B(X) - 20 \log \frac{d_B(X)}{d_A(X)} \quad (1)$$

where the above expression reflects removal of inverse-square radiation effects.

The above process can be repeated for a number of radiation angles. Thus, in the analysis, differences were determined for radiation angles at 5° intervals extending from 30° (as measured from the forward direction of the aircraft) to 150°.

Some limitations in analysis are evident by study of Fig. 1. Signal losses by propagation over very large distances limit the useful data at very large or very small radiation angles. Also, as shown in Fig. 2, the signals received at positions other than those directly underneath the aircraft are received at elevation angles which are smaller than the radiation angle. For example, for a flyover at 1000 ft, a signal radiated from the aircraft at an angle of 30° with respect to the flight path would be received at a ground position located 2000 ft to the side of the flight path at an elevation angle of about 13°.

For small elevation angles, there is the increased likelihood of bending of propagation paths, and increased scattering due to longer path lengths through the lower layers of the atmosphere. Thus, in processing the noise data, all noise levels received at elevation angles of 20° or less were arbitrarily excluded from the analysis.



## MEASUREMENT PROGRAM

### Description of Field Measurements

The measurements were made at NASA-Wallops Station, Virginia on April 29, 1969. Seven flights of the four-engine turbojet aircraft at altitudes of 1500 and 2000 ft were recorded in the morning. In the afternoon, six flights of the four-engine piston aircraft at altitudes of 700 and 1500 ft were recorded, followed by seven flights of the four-engine turbojet at altitudes of 1500 and 2000 ft. Table I lists the flights and the basic parameters of altitude, air speed and engine settings as reported by the flight crew.

The pilots were instructed to accept some speed variation but to hold altitude and engine power setting constant along the prescribed flight path. The aircraft were tracked along the major portion of the useful flight track with a ground-based Bell Aerosystem GSN-5 localizer and position unit. Time markers were placed manually on the altitude and flight track traces from the radar unit, based upon radio transmission of audio time signals at approximate 15 second intervals throughout the flight. The transmitted audio time signals were also recorded at each noise measurement position.

Noise signals were recorded at the five positions shown in Fig. 3. This figure shows the location of the measurement positions with respect to the aircraft flight path and approximate limits of the radar tracking data.

Measurement positions were selected so that the same type of ground cover (grass) existed at each site. The noise measurement instrumentation, outlined in block form in Fig. 4, was similar at each position.

As indicated in Fig. 4, the flyover noise signal for each microphone was recorded at each station on two channels of an FM tape recorder, one channel having conventional flat frequency response. For the second channel, a low frequency de-emphasis network and additional amplification were added to obtain recorded signals having increased signal-to-noise ratios at high frequencies. Only data recorded on the second channel was used in the atmospheric absorption analysis.

#### Meteorological Measurements

In support of the flight measurements, a series of special radiosonde ascents were made, commencing 30 minutes before the first flights in the morning and terminating at the conclusion of the afternoon flights. During this period, temperature, winds and pressure at the surface were continuously monitored and recorded by standard U. S. Weather Bureau (USWB) instruments at the end of the runway. Surface temperature and humidity were also continuously monitored at one of the noise measurement positions to the side of the runway. The radiosondes were standard USWB units modified to obtain either temperature or humidity only. Vertical wind profile data were obtained by double-theodolite tracking. Data from the radiosondes were read out at 15-second intervals resulting in a mean vertical spacing of temperature or humidity data at approximately 300 ft intervals. The radiosondes were

further modified to terminate transmission after approximately 5000 ft of ascent, making it possible to launch successive radiosondes at time intervals of less than 30 minutes.

A detailed description of the weather conditions existing during the time of the measurements is presented in Appendix A. Table II shows the average surface temperature and humidity during the three sets of flyovers. The table also lists the range of surface temperatures, relative humidities, wind speeds and barometric pressures during the elapsed time period for the measurements. Figures 5 and 6 show plots of the temperature and absolute humidity as a function of time from mid-morning to late afternoon. Figure 7 shows a plot of the temperature and absolute humidity profiles as a function of altitude existing at the time of the morning measurements. Based on the temperature ranges observed at the surface and aloft to 2000 ft height, the speed of sound ranged from 1015 to 1025 ft per second during the flyovers.

The tests were conducted during a day of changing weather conditions although surface temperatures, humidity and winds did not show large variations throughout the day. A mild temperature inversion existed at the time of the morning measurements (see Fig. 7) which later disappeared with surface heating. A frontal passage occurred near or shortly following the time of the morning measurements.

#### Noise and Aircraft Data Analysis

For each flyover, noise and operational data were studied as follows:

- a) The position of the aircraft was determined as a function of time from the radar tracking information.
- b) The noise signals recorded on the ground were analyzed in one-third octave frequency bands at half-second intervals.
- c) By time correlation of the noise spectra at different ground locations with the position of the aircraft and consideration of differences in propagation distances, values of atmospheric absorption as a function of propagation distance were determined.

Figure 8 illustrates the major steps in the data analysis process in block form.

From the x-y plots of altitude and flight track produced by the radar unit, together with time marks, the altitude, lateral displacement and distance along the flight track of the aircraft were determined as a function of time. Using this information and an average value for the speed of sound, the times at which the noise signal radiating from the aircraft at various radiation angles would be received at each of the ground measurement positions were computed. (A brief description of the computations utilized during the data analysis may be found in Appendix B.) Also calculated were the propagation distances from the aircraft to each of the ground locations, corresponding to the propagation paths for the various angles of radiation.

A separate step in the study is the analysis of the noise signal received at each ground location. This was accomplished by playback of the noise signals recorded with low frequency de-emphasis into a Hewlett-Packard Real Time Audio Spectrum Analyzer. Under the control of a Digital Equipment PDP-8 computer, the noise signals were analyzed by the Spectrum Analyzer at half-second intervals in one-third octave frequency bands extending from 50 Hz to 10,000 Hz center frequencies, with one of the time signals recorded on the annotation channel of the tape used as a time reference. Acoustic calibration signals, recorded on the tape at the time of the field experiment, were utilized as a check on system performance and as a calibration standard for the noise signals. In addition, frequency response corrections, determined from the frequency characteristics of the record and playback systems, were applied to the data.

The output of the PDP-8 computer was a paper tape, on which noise spectra at half-second intervals were coded in digital form. The paper tape was read into an IBM Paper Tape Reader/Punch connected to an IBM 360-30 computer, which transferred the data from paper tape onto punched cards for further computer processing.

Using the times, calculated previously, when the noise signals would be received on the ground as a function of radiation angle, the noise levels in each frequency band\* at the different ground locations for the various radiation angles were determined by interpolation of the half-second noise data.

---

\* For the purposes of this study, only data in one-third octave frequency bands from 400 Hz to 10,000 Hz center frequencies were considered.

In each frequency band the noise floor was established by visual examination of the time histories of the noise signals, plotted by the computer. The noise floor values were used to adjust the noise levels for signal-to-noise ratio effects, and to invalidate noise data that were within three decibels of the noise floor.

Then, the atmospheric absorption was obtained for each radiation angle and frequency band under consideration by taking the difference in adjusted noise levels observed at each position pair, and removing the values of inverse-square attenuation calculated earlier in accord with Eq. (1). The resulting output was a listing, for each radiation angle, of incremental propagation distances and the corresponding values of atmospheric absorption as a function of frequency.

## MEASUREMENT RESULTS

### Calculated Atmospheric Absorption

Atmospheric absorption values were computed from SAE ARP 866 curves or tables for field temperature and humidity data at 200 ft intervals from surface to 2000 ft altitude for each of the three periods of noise measurements. Table III lists the mean SAE ARP 866 values for each of the three measurement periods based upon averaging absorption values between the surface and 1500 ft altitude.

The differences among the three average curves are quite small, ranging from 0.1 dB per 1000 ft at 1000 Hz, and 0.6 dB at 4000 Hz, to a maximum of 2.0 dB at 8000 Hz. Table III also lists a mean set of absorption values computed from the averages for the three sets of flyovers. In later figures, this mean set of values will be taken to represent values obtained by SAE ARP 866 calculations.

Table III also shows a set of mean absorption values computed from only surface measurements of temperature and humidity during the flyovers. Differences between these values and the mean computed from surface and altitude data are very small, ranging from 0.1 dB per 1000 ft at frequencies of 3150 Hz or less, to a maximum difference of 0.4 dB per 1000 ft at 8000 Hz.

The mean absorption values computed from surface and altitude measurements (from Table III) are shown in Fig. 9 together with the maximum and minimum values calculated for any surface or 200 ft altitude interval (to 2000 ft) condition existing during the flyover measurements. The total range in absorption values is, of course, considerably larger than the range between averages for the three sets of flyovers.

The maximum range in absorption values during any one set of flyover measurements occurred during the afternoon turbojet aircraft flyovers, where maximum spreads in calculated values with altitude ranged from 0.2 dB per 1000 ft at 1000 Hz, and 1.5 dB at 4000 Hz, to 8.0 dB at 8000 Hz.

It should be noted that the tests were conducted under high humidity conditions, in the range where calculated atmospheric absorption values are quite insensitive to small changes in temperature or humidity. Had the tests been conducted under lower humidity conditions, the measured variations in temperature and humidity could have produced much larger variations in calculated atmospheric absorption.

#### Measured Atmospheric Absorption Values

Figures 10 and 11 show typical plots of the excess attenuation in dB vs propagation distance in feet. The figures show data for an afternoon run of the turbojet for frequencies of 1000 and 4000 Hz. Data symbols in the figures distinguish between data obtained while radar tracking data was available and data acquired by extrapolation beyond the limits of radar tracking (which occurs primarily at large radiation angles). Data received at elevation angles at ground positions of less than 20 degrees are excluded.

The slopes of linear regression lines fitted to the experimental data yield experimental values of atmospheric absorption in dB per 1000 ft. In analysis, three types of least squares regression line fits to the experimental data were considered: (a) unweighted regression lines, (b) weighted regression lines with the weighting linearly proportional to the differential propagation distance. and (c) weighted regression lines with



the regression lines forced to pass through the x- and y-axis intercept.\* Figures 10 and 11 show examples of the three regression lines fitted to a set of flyover data.

It was generally found that, as indicated in Figs. 10 and 11, the slopes of the regression lines (and hence, the atmospheric absorption values) were not particularly sensitive to nor dependent upon the type of regression line analysis. This is further illustrated in Fig. 12 which shows the average absorption values determined for the seven afternoon flyovers of the turbojet transport aircraft. The three curves show the absorption values determined from the unweighted, weighted and forced-weighted regression line analysis. Comparison of the standard deviations for the mean values shown in Fig. 12 indicates there was slightly less variability at a given frequency for the weighted regression line. However the differences in variability were not large.

In choosing data for later presentation, an arbitrary choice was made to rely primarily upon the absorption values determined from weighted regression lines. In comparison with the unweighted regression line, this data gives greatest weight to differences in noise levels observed for large propagation path differences where one would most reasonably expect the differences in noise levels to be due to absorption effects rather than various possible experimental errors.\*\*

---

\* The different equations for determining the regression lines are given in Appendix B.

\*\* In some cases we will utilize statistical analysis based upon unweighted regression lines, primarily for the ease of statistical interpretations utilizing unweighted regression lines.

Figures 13, 14 and 15 show the absorption values determined from the slopes of weighted linear regression lines calculated from data for each individual flyover. In the figures, each flight is denoted by a separate symbol. As shown by the coding of the symbols there were often considerably fewer data samples at high frequencies. The lessened number of data samples at high frequencies is due to the decreasing signal-to-noise ratio at high frequencies which eliminated useful data at both large and small radiation angles. Also shown in each figure is the average absorption based upon SAE ARP 866 calculations, previously shown in Fig. 9.

Mean values\* of the atmospheric absorption determined for each of the three sets of flyover measurements shown in Figs. 13, 14 and 15 are shown in Fig. 16. Also shown in this figure is the mean atmospheric absorption value calculated from SAE ARP 866. One will note that the experimental data lies slightly above the calculated curve for frequencies below 1000 Hz. The experimental data brackets the SAE values in the frequency range from about 1000 to 4000 Hz; the turbojet data falls below the SAE values at frequencies above 5000 Hz while the propeller aircraft data stays consistently above the SAE value at frequencies of 4000 Hz and above.

The data presented in Fig. 13 through 16 have utilized data obtained when accurate tracking data was available and have also included data when tracking information and aircraft position was obtained by extrapolation beyond the range of the radar information. When such extrapolated

---

\* In determining the mean value for a set, values for an individual flyover were weighted in accord with the number of data points used to determine the individual flyover values.

data is removed and regression lines are recalculated, some differences appear, particularly for the turbojet data. Figure 17 shows the average data for each of the three sets of flyover measurements with extrapolated data removed. In comparison with Fig. 16 the data of Fig. 17 shows slightly higher atmospheric absorption values for the turbojet data at frequencies of 2000 Hz or less. Also the atmospheric absorption values are higher in the range from 4000 Hz and above. As a consequence the spread among the three sets of experimental data is reduced at 4000 Hz and higher frequencies.

To further explore possible variables effecting the experimental absorption values, regression lines were calculated for the data obtained only for flyovers at 1500 ft (eliminating the data for flights at 700 ft for the piston aircraft and for flights at 2000 ft for the turbojet aircraft). Figure 18 shows the mean absorption coefficients determined from weighted regression lines for the three sets of flyovers at altitudes of 1500 ft. Comparison with Fig. 17 will indicate little change in the data for the turbojet aircraft and relatively little change for the piston aircraft for frequencies below 4000 Hz. However above 4000 Hz the absorption values from the piston aircraft are lower and now are very close to those measured with the turbojet aircraft.

To facilitate comparisons between the data presented in Figs. 16, 17 and 18, average absorption curves were calculated for each of the three sets of absorption values shown separately in three figures. These averaged values are tabulated in Table IV and are also plotted in Fig. 19 for comparison with the average SAE ARP 866 values.

From Fig. 19 one notes that all three field curves follow the calculated SAE curve within about  $\pm$  one dB from 1000 Hz to 5000 Hz. At frequencies below 1250 Hz, all three experimental curves consistently yield higher absorption values than predicted by SAE ARP 866. At high frequencies, the experimental curves follow the slope of the calculated curve well, except at 8000 Hz.

Figure 19 indicates that, among the three experimental curves, elimination of extrapolated tracking data points results in a general, slight increase in atmospheric absorption values. Little difference is noted between data for all flights and only 1500 ft flights (extrapolated data removed) except at 8000 Hz.

A study was undertaken to see if there was significant differences in experimental atmospheric absorption values due to variations with angle of radiation from the aircraft. For this analysis, data was divided into three groups -- angles of radiation of  $30^\circ$  to  $65^\circ$ ,  $70^\circ$  to  $110^\circ$  and  $115^\circ$  to  $150^\circ$ . (With elimination of the data obtained beyond the range of accurate radar tracking, there was considerably less turbojet data for the angle range from  $115^\circ$  to  $150^\circ$ .)

The piston aircraft curves, shown in Fig. 20, show little consistent difference in absorption values among the three angle groupings. However, for the turbojet aircraft curves, shown in Fig. 21 (and based upon data for both morning and afternoon flyovers), the curve for radiation angles from  $115^\circ$  to  $150^\circ$  is consistently lower than the curves for the other two angle groupings.

If one were to determine absorption values using only the maximum levels occurring in each one-third octave band during a flyover - a technique often used previously in obtaining estimates of atmospheric absorption from flyover noise records - the results for turbojet aircraft would be based, typically, on the noise radiated at angles from about  $120^\circ$  to  $150^\circ$ . Thus, this technique applied to the turbojet data under study would yield absorption values lower than that obtained by utilizing data from a wider range of radiation angles.

#### Measurement Variability

As discussed previously, there may be considerable fluctuation in noise signals propagated over large distances. In addition, the time-varying levels of a flyover noise signal together with changes in angle of sound radiation and propagation distance with time do not permit averaging flyover sound levels over long time intervals to improve accuracy of measurement. As an alternate to long time samples, one may achieve increased accuracy by ensemble averaging, utilizing the data from a number of measurements at different microphone positions or through repeat flyovers, provided other conditions of the test remain unchanged.

To obtain estimates of the variability in the flyover measurements, two different measures of variability were studied. One measure was obtained by determining the confidence intervals for the slopes of the (un-weighted) regression lines fitted to the basic data as shown in Fig. 10 and 11. Application of standard statistical methods (Ref. 6), and assuming normal distributions yields measures

of the confidence intervals which may be assigned to the slopes of the regression lines. Such statistical analysis for data from a single typical turbojet flyover indicates 95% confidence intervals ranging from about  $\pm 1$  dB per 1000 ft for frequencies at 2500 Hz or less increasing to the order of  $\pm 2$  dB and greater at frequencies above 5000 Hz.

Grouping together data from repeat flyovers will reduce the confidence intervals and results in increased assurance of measurement accuracy. The 95% confidence interval for mean values, determined by grouping together all data for one set of six (or seven) flyovers showed a minimum confidence interval of  $\pm 0.32$  dB per thousand feet (occurring at 2500 Hz for the piston aircraft flyovers) and a maximum confidence interval of  $\pm 2.2$  dB (occurring at 8000 Hz for the piston aircraft flyovers).

Computing root-mean square values of the confidence intervals for all frequencies from 400 to 6300 Hz yielded interval values of  $\pm 0.59$  dB and  $\pm 0.41$  dB for the morning and afternoon turbojet flights respectively and  $\pm 0.46$  dB for the afternoon piston aircraft flights. These values indicate more variability for the morning data, but little difference in variability for the two sets of afternoon flights.

If one considers the 95% confidence interval of  $\pm 0.6$  dB per thousand feet as representative of the value in any frequency band of any one set of data, differences between sets of data of about one dB per thousand feet or more would be considered statistically significant at the 95% confidence level. With a 95% confidence interval of  $\pm 2$  dB for the average slope value a difference of about 3 dB or greater

would be significant at a 95% confidence interval. On this basis, the differences between the three curves of Fig. 19 would not be statistically significant at the 95% confidence level.

A different measure of variability can be determined by comparing the noise levels in a given frequency band observed at the same ground position for the same angle of radiation from the aircraft during repeat flyovers of the aircraft at the same altitude. Table V summarizes the results of such an analysis, undertaken for data received at Position 2 (the position directly underneath the flight path) and for Position 5, the position furthest from the flight path for the turbojet flyovers at 2000 ft altitude during the morning and afternoon.

Mean levels and standard deviations for the means were determined for each angle at 5° intervals of radiation angle at frequencies of 500, 1000, 2000, 4000 and 6300 Hz. The table lists the mean standard deviation for a given frequency band irrespective of distance for Position 2 and for Position 5.\* Table values show an increase in the standard deviation with frequency; also, greatest variability is observed for measurements at Position 5.

The standard deviations plotted as a function of propagation distance generally show an increase in size with increased propagation distance for the levels measured directly under the aircraft (Position 2); however this trend is not consistent for the data at Position 5. To

---

\* The variability in noise levels for any one-third octave frequency band at a given angle will generally be larger than the variability in a flyover noise level measure based upon a broader frequency bandwidth, or a flyover measure calculated from a number of band level measurements. Thus the flyover noise measures reported in Ref. 7 for the same flyover data will show considerably less variability than the data discussed here.

illustrate the trend with distance observed at Position 2, Fig. 22 shows the standard deviations for frequencies of 1000 and 4000 Hz plotted as a function of propagation distance. Typically, at 4000 Hz, the standard deviation increases from about 1 dB at 2000 ft to about 3 dB at 4000 ft propagation distance.

#### Signal-to-Noise Limitations at High Frequencies

The number of experimental values of sound absorption used to determine the regression lines (see Fig. 10 and 11) was essentially constant over the frequency range from 400 to 5000 Hz but decreased at 6300 Hz with a more marked decrease at 8000 Hz, primarily as a result of degradation in signal-to-noise ratios. To determine the degree of improvement achieved in practice by utilizing the low frequency de-emphasis circuit in recording (see Fig. 4) and to determine the extent of potential future improvements which might be possible before reaching limits set by ambient acoustic noise levels, background noise levels were measured at the output of the data reduction system (the output from the PDP-8 computer of Fig. 8). Table VI lists these background noise levels for both the conventional flat system and the channel with the low frequency de-emphasis circuit. In addition the table lists estimates of the ambient acoustic noise level existing on the site and the typical electrical background levels at the output of the microphone cathode follower. All levels are stated in terms of the equivalent input sound pressure levels to a typical 1/2 inch condenser microphone.

Comparison of the levels given in Table VI indicates that the low frequency de-emphasis circuit resulted in a reduction of equivalent noise floor levels of 14 dB at



5000 Hz and 20 dB at 8000 Hz. However, even with the de-emphasis circuit, instrumentation noise levels are of the order of 25 to 30 dB above estimated ambient acoustic levels or the background signal level at the output of the microphone cathode follower at 8000 Hz. This comparison clearly indicates the potential for further changes in instrumentation to achieve lower effective background levels with promise of considerable improvement before being limited by system input noise levels.

## CONCLUSIONS

This comparison of atmospheric absorption values obtained from flyover noise measurements with calculated absorption values based upon temperature and humidity measurements at the surface and aloft provides the following conclusions:

1. The data analysis techniques employed in this study yield useful atmospheric absorption values over the frequency range up to 8000 Hz. Moderate accuracy in determining absorption values resulted from data for a single flyover. Significantly better accuracy can be obtained by grouping data from several flyovers, thus for sets of 6 or 7 flyovers typical 95% confidence intervals of  $\pm 0.4$  to 0.6 dB per 1000 ft were obtained for atmospheric absorption values over the frequency range from 400 to 6300 Hz.
2. The tests were conducted under conditions of high humidity and moderate temperature in a range where atmospheric absorption is not sensitive to small changes in either temperature and relative humidity. For the single day of measurements the differences between calculated mean sound absorption values based only upon surface measurements of temperature and humidity and calculated mean values using combined surface and altitude measurements of temperature and humidity were small, ranging from 0.1 dB per 1000 ft at frequencies of 3150 Hz or less to a maximum of 0.4 dB per 1000 ft of 8000 Hz. However, the calculated absorption at various altitudes did show moderate variation from mean values. This variation indicates the desirability of making both surface and altitude measurements of temperature and

humidity in order to determine the extent of possible atmospheric absorption variations during field measurements.

3. For the very limited set of meteorological conditions encountered during the tests, the mean atmospheric absorption values obtained from combined data for the three sets of flyover measurements shows good agreement with SAE ARP 866 calculated values over the frequency from 1250 Hz to 6300 Hz. At 1000 Hz and lower frequencies (to 400 Hz, the lower limit of the analysis) the experimental values, typically averaging 2 dB per thousand feet, are significantly greater than the calculated values. This increase in absorption at lower frequencies may reflect losses due to scattering in the lower atmosphere not accounted for in the current industry calculation procedures.

Considerable spread in experimental absorption values at 8000 Hz and inconsistent agreement with calculated values reflects, in part, the lessened accuracy in field measurements due to sharp reductions in data sample sizes at 8000 Hz.

4. Comparison of the experimental absorption values for flyovers of the four-engine propeller transport aircraft with those from the four-engine turbojet transport aircraft yielded generally comparable data with no consistent difference, except as follows:

- (a) At 8000 Hz the propeller aircraft flyovers provided higher atmospheric absorption values than the jet aircraft data. This finding may not be significant due to the limited accuracy in field data at 8000 Hz.

- (b) Comparison of measured absorption values for different angles of radiation from the aircraft showed no consistent difference in absorption values for the propeller aircraft data. However, for the jet aircraft, absorption values for large radiation angles (115 to 150° from the forward flight axis) showed consistently lower values over the entire frequency range than for smaller radiation angles or the values obtained from the propeller aircraft flyover data. If this trend is consistent for other jet aircraft, it may help explain the reason for the reported field absorption values from aircraft flyover measurement that are often lower than those based on SAE ARP 866 calculations.

5. The field measurement and data analysis techniques utilized in this study appear applicable for further studies of atmospheric absorption utilizing flyover measurements conducted over a wider range of temperature and humidity conditions. Improvements in field measurements are recommended in order to obtain increased accuracy of measurements particularly at the higher frequencies to 10,000 Hz:

- (a) Surface measurements of temperature and humidity and winds should be made at each ground position. In addition, it would be desirable to obtain near-simultaneous radiosonde measurements of temperature and humidity during the field measurements instead of alternate measurements of temperature and humidity as done in the current tests.

- (b) Radar tracking limits with respect to ground noise measurement positions should be carefully adjusted in order to obtain accurate radar information over a larger segment of the useful flight path.
- (c) The noise data acquisition and data reduction instrumentation should be reviewed and changes incorporated in order to improve the useful signal-to-noise ratio in the frequency range covering the 5000 to 10,000 Hz one-third octave bands. Considerable reductions in equivalent background noise levels are possible without being limited by ambient acoustic noise levels or microphone/cathode follower electrical background noise limits.

## REFERENCES

1. Anon: Standard Values of Atmospheric Absorption as a Function of Temperature and Humidity for Use in Evaluating Aircraft Flyover Noise. Soc. Automotive Engrs. ARP 866, August 1964.
2. Robinson, D. W.; Copeland, W.C.T: Interim Proposal for Air Attenuation Values for Aircraft Noise. NPL Aero-Report AC28, British A.R.C. 29, 276, July 1967.
3. Hale, R. T.; An Investigation into Atmospheric Absorption using B.A.C. Air to Ground Measurements. British Aircraft Corp. Acoustics Report 156, Issue 2, October 1968.
4. Little, John W.; Miller, Robert L.; Oncley, Paul B.; and Panko, Raymond E.: Studies of Atmospheric Attenuation of Noise. NASA Acoustically Treated Nacelle Program, NASA SP-220, pp. 125-135, October 1969.
5. Federal Aviation Regulations, Part 36: Noise Standards: Aircraft Type Certification. 1969.
6. Crow, Edwin L.; Davis, Frances A; and Maxfield, Margaret W.: Statistics Manual. Dover Publications (New York), 1960.
7. Bishop, Dwight E.: Variability of Flyover Noise Measures for Repeated Flights of Turbojet and Piston Engine Transport Aircraft. NASA CR-1752, 1971.

TABLE I  
LOG OF AIRCRAFT TEST FLIGHTS - 29 APRIL 1969,  
NASA, WOLLOPS STATION, VIRGINIA

A/C	Flight No.	Time EDST	Alt, ft	IAS, Kn	A/C gross Wt, 1000 lbs	Engine Settings
880	111	0630	1500	208	143.1	EPR 2.2
	112	0639	1520	205	140.3	2.2
	113	0645	1530	205	138.5	2.2
	114	0652	1975	204	136.4	2.2
	115	0659	2050	202	133.7	2.2
	116	0707	2100	205	131.5	2.2
	117	0714	1500	203	129.6	2.2
880	211	1641	1500	210	150.5	EPR 2.2
	212	1648	1550	198	148.3	2.2
	213	1655	1500	208	146.2	2.2
	214	1703	2200	208	142.9	2.2
	215	1710	2100	204	141.2	2.2
	216	1718	2050	205	139.7	2.2
	217	1728	2000	208	133.5	2.2
1049G	221	1517	700	220	101.6	BMEP 234,2600 RPM
	222	1524	700	220	100.8	234,2600
	223	1531	700	220	100.0	234,2600
	224	1538	1500	220	99.2	234,2600
	225	1546	1500	220	98.4	234,2600
	226	1553	1500	220	97.6	234,2600

TABLE II  
TYPICAL SURFACE WEATHER PARAMETERS DURING FLIGHTS

Time EDST	A/C	Flt No.	Temp °F	R.Hum. %	Wind Speed, Kn	Bar. Press Press in Hg.
0630 0720	880	111- 117	58 58.5	100 100		
1515 1600	1049G	221- 226	61 59.5	85 88		
1640 1730	880	211- 217	59.5 59.5	88 80		
0630 to 1730		Max Min	70 57	100 67	9.5 0	29.89 29.85



TABLE III  
AVERAGE ATMOSPHERIC ABSORPTION VALUES BASED  
UPON SAE ARP 866 CALCULATIONS

One-third Octave Band Frequency, Hz	Atmospheric Absorption in dB per 1000 ft				
	Surface and Altitude Data*				Surface Data Only**
	Turbojet Morning	Piston Afternoon	Turbojet Afternoon	Average (3 sets)	Average (3 sets)
400	0.6	0.6	0.6	0.6	0.7
500	0.7	0.7	0.7	0.7	0.8
630	0.9	0.9	0.9	0.9	0.9
800	1.2	1.1	1.2	1.2	1.2
1000	1.5	1.4	1.4	1.4	1.5
1250	1.8	1.9	1.8	1.8	1.9
1600	2.4	2.3	2.4	2.4	2.4
2000	3.0	3.0	2.9	3.0	3.0
2500	3.8	3.9	3.9	3.9	4.0
3150	4.9	5.0	5.0	5.0	5.1
4000	6.4	7.0	6.7	6.7	6.9
5000	7.4	8.0	7.8	7.7	7.9
6300	10.1	11.0	10.8	10.8	10.8
8000	14.0	16.0	15.3	15.1	15.5

\* Values reported for each flyover set are based upon average of atmospheric absorption values determined from temperature and humidity at the surface and at 200 ft intervals aloft to an altitude of 1500 ft.

\*\* Based only on surface measurements during the three sets of flyover measurements.

TABLE IV  
AVERAGE EXPERIMENTAL ATMOSPHERIC ABSORPTION  
VALUES FOR FLIGHTS ON APRIL 29, 1969\*

One-third Octave Band Frequency, Hz	ATMOSPHERIC ABSORPTION, dB per 1000 ft		
	All Data (Fig. 17)	No Extrapolated Tracking Data (Fig. 18)	1500 ft Flights, No Extrap. Tracking Data (Fig. 19)
400	1.8	2.7	2.5
500	1.7	2.4	2.7
630	1.7	2.2	2.4
800	1.9	2.4	2.6
1000	1.5	2.0	2.4
1250	1.6	2.0	2.4
1600	1.9	2.3	2.7
2000	2.6	2.9	3.1
2500	3.4	3.8	3.9
3150	5.0	5.5	5.7
4000	6.5	7.1	7.3
5000	8.1	8.8	9.0
6300	10.1	11.5	11.1
8000	11.4	12.9	10.5

\* Values listed are the average of the values determined individually for the three sets of flyover measurements on April 29, 1969.

TABLE V  
TYPICAL STANDARD DEVIATION FOR SOUND LEVELS\* MEASURED  
DURING REPEAT FLYOVERS OF FOUR-ENGINE TURBOJET AIRPLANE  
AT NOMINAL 2000 FT ALTITUDE

Position**	Propagation Distance Range Ft	Standard Deviation in dB				
		One-Third Octave Frequency Band in Hz				
		500	1000	2000	4000	6300
2	1880 to 3840	0.8	0.9	1.0	1.5	2.2
5	2650 to 5500	2.4	2.8	2.9	3.8	2.8

\* One-third octave band sound levels observed at 5 degree intervals over radiation angles of 30° to 150° for seven flyovers. The rms standard deviation,  $\bar{s}$  was computed as follows:

$$\bar{s} = (s_{30^\circ}^2 + s_{35^\circ}^2 + s_{150^\circ}^2)^{1/2}$$

where  $s_\theta$  is the standard deviation for band levels at radiation angle  $\theta$ .

\*\* See Figure 3.

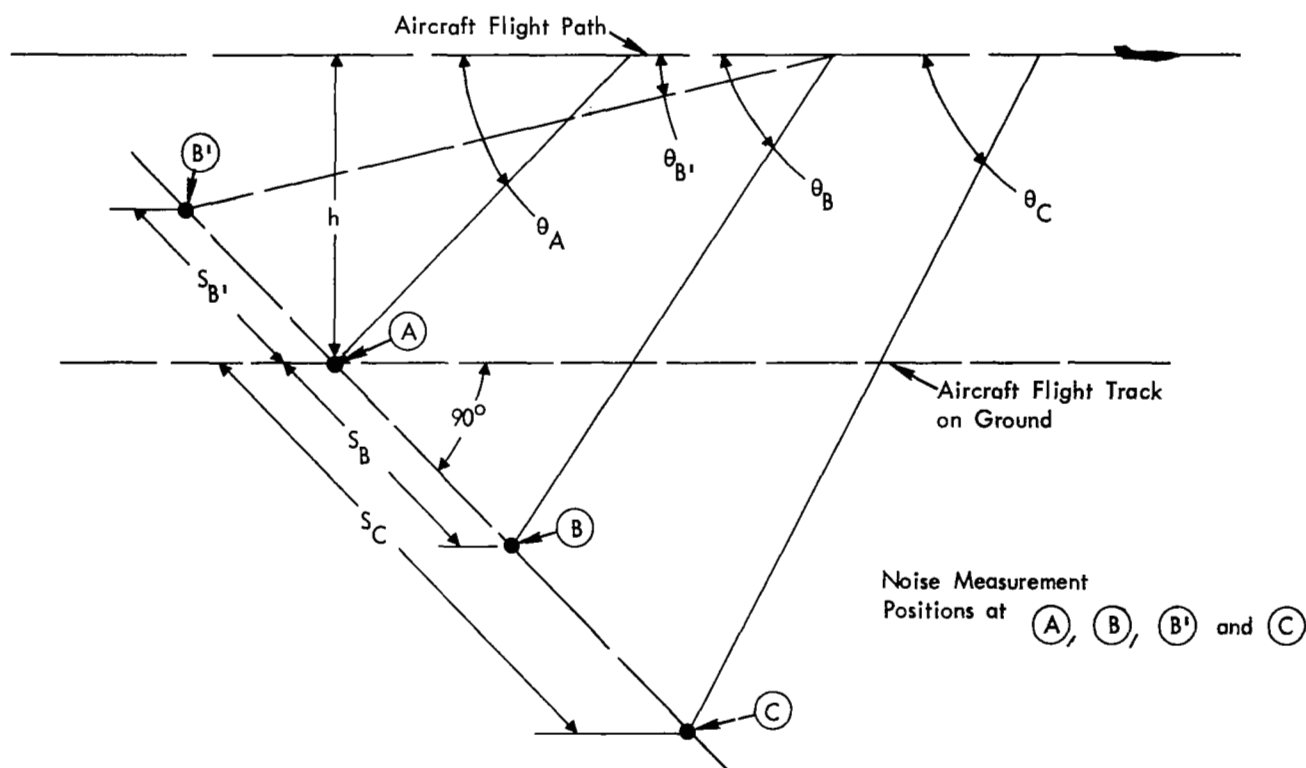


FIGURE 1. SKETCH OF IDEALIZED MEASUREMENT ARRANGEMENT FOR STUDY OF AIR-TO-GROUND SOUND PROPAGATION

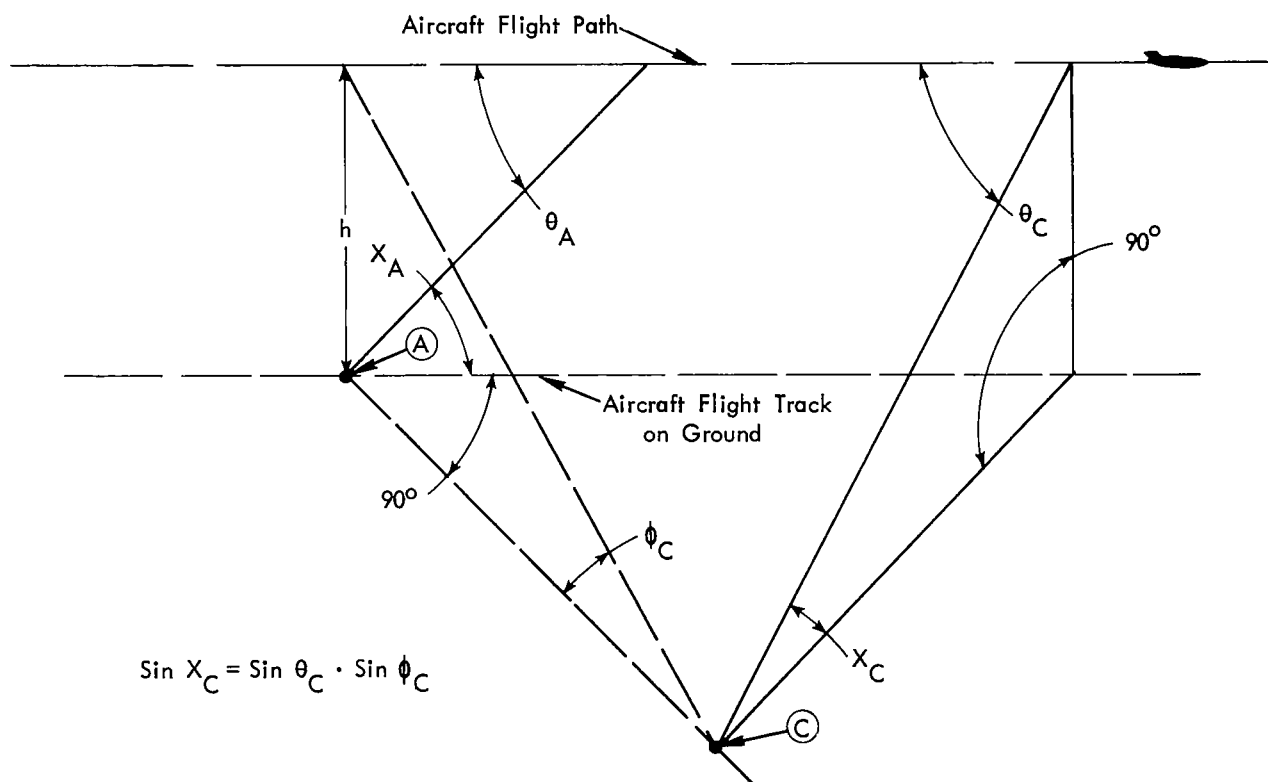


FIGURE 2. SKETCH OF MEASUREMENT SETUP SHOWING LIMITING ELEVATION ANGLES

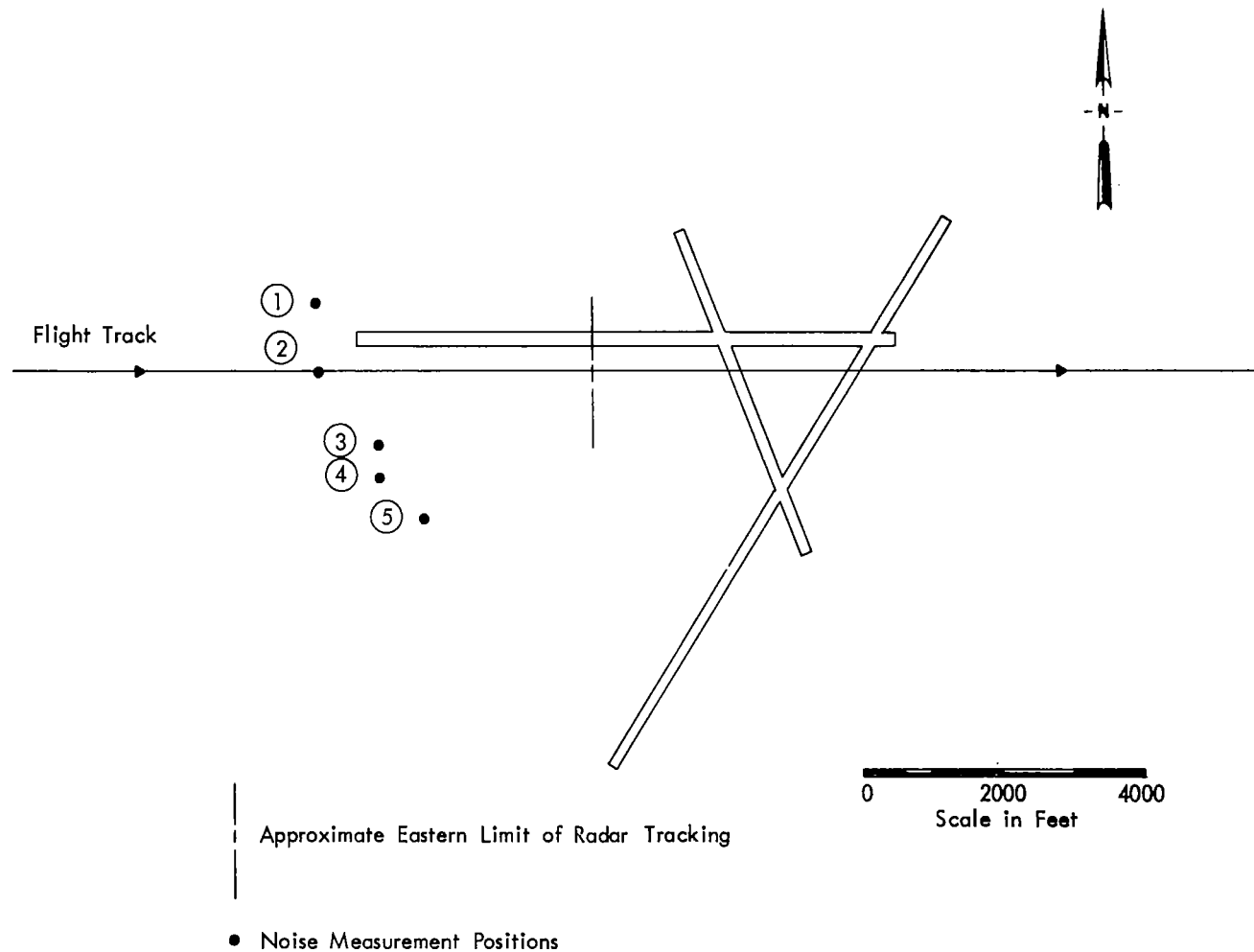
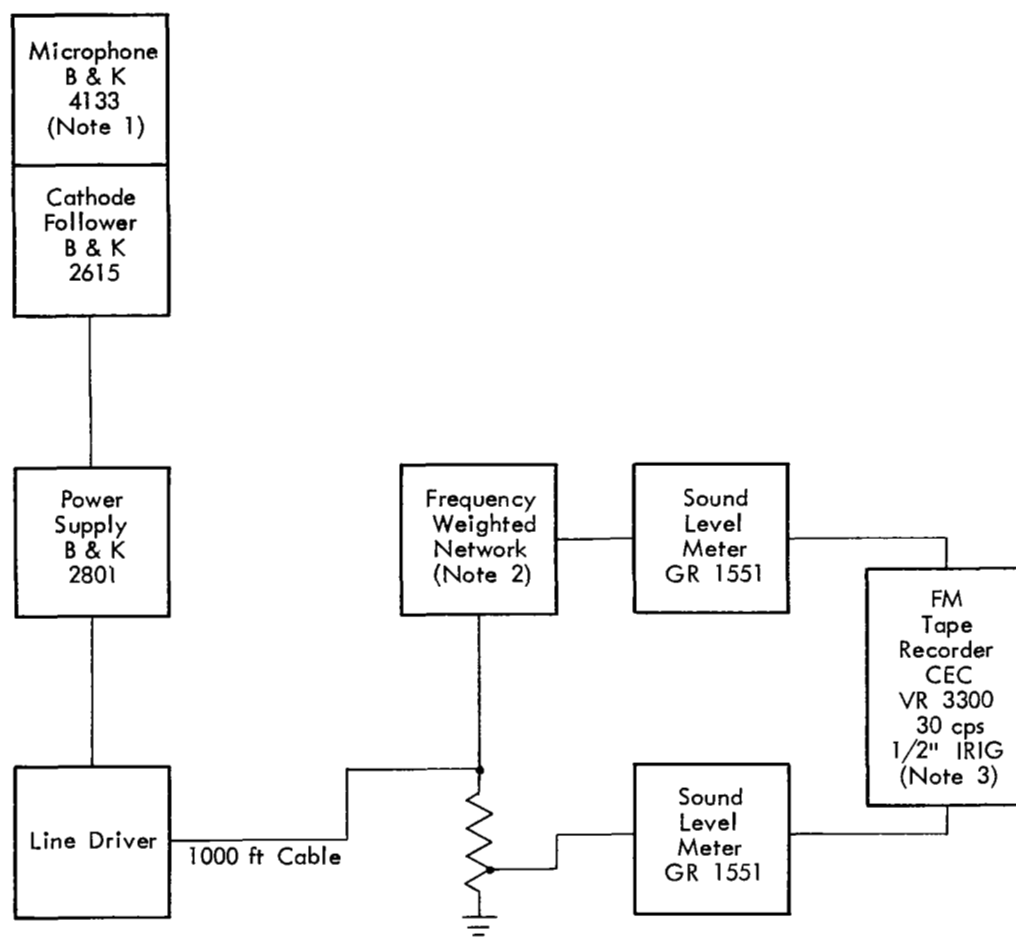


FIGURE 3. LOCATIONS OF NOISE MEASUREMENT POSITIONS WITH RESPECT TO AIRCRAFT PATH



NOTES:

1. Microphone placed 1.2 m (5 ft) above ground with diaphragm perpendicular to flight path.
2. High-pass filter, -36 dB atten at 100 Hz, -6 dB atten at 20 kHz.
3. Voice time synchronization signal (from central station) recorded on separate channel

FIGURE 4. TYPICAL FLYOVER NOISE MEASUREMENT INSTRUMENTATION

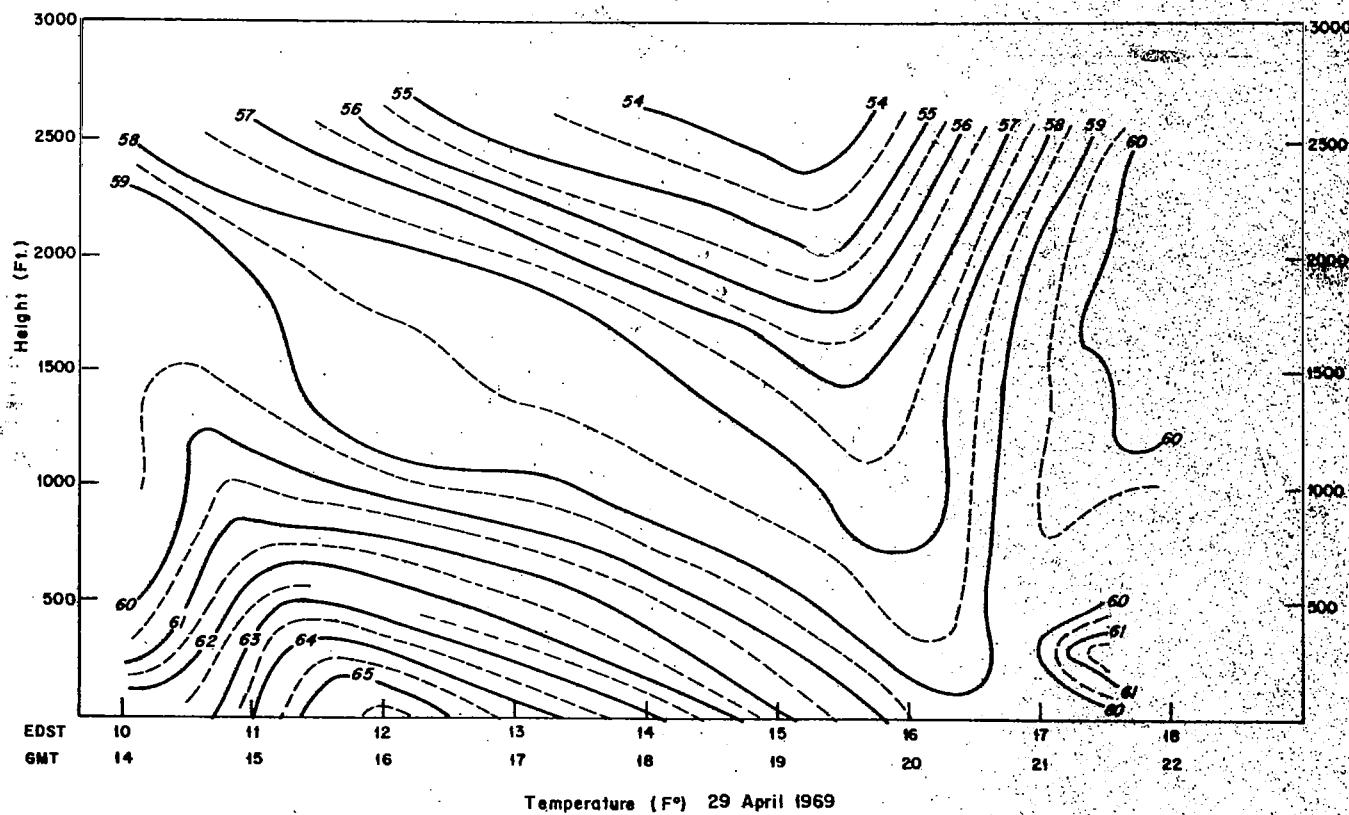


FIGURE 5. TEMPERATURE VARIATIONS DURING AFTERNOON FLYOVER MEASUREMENTS



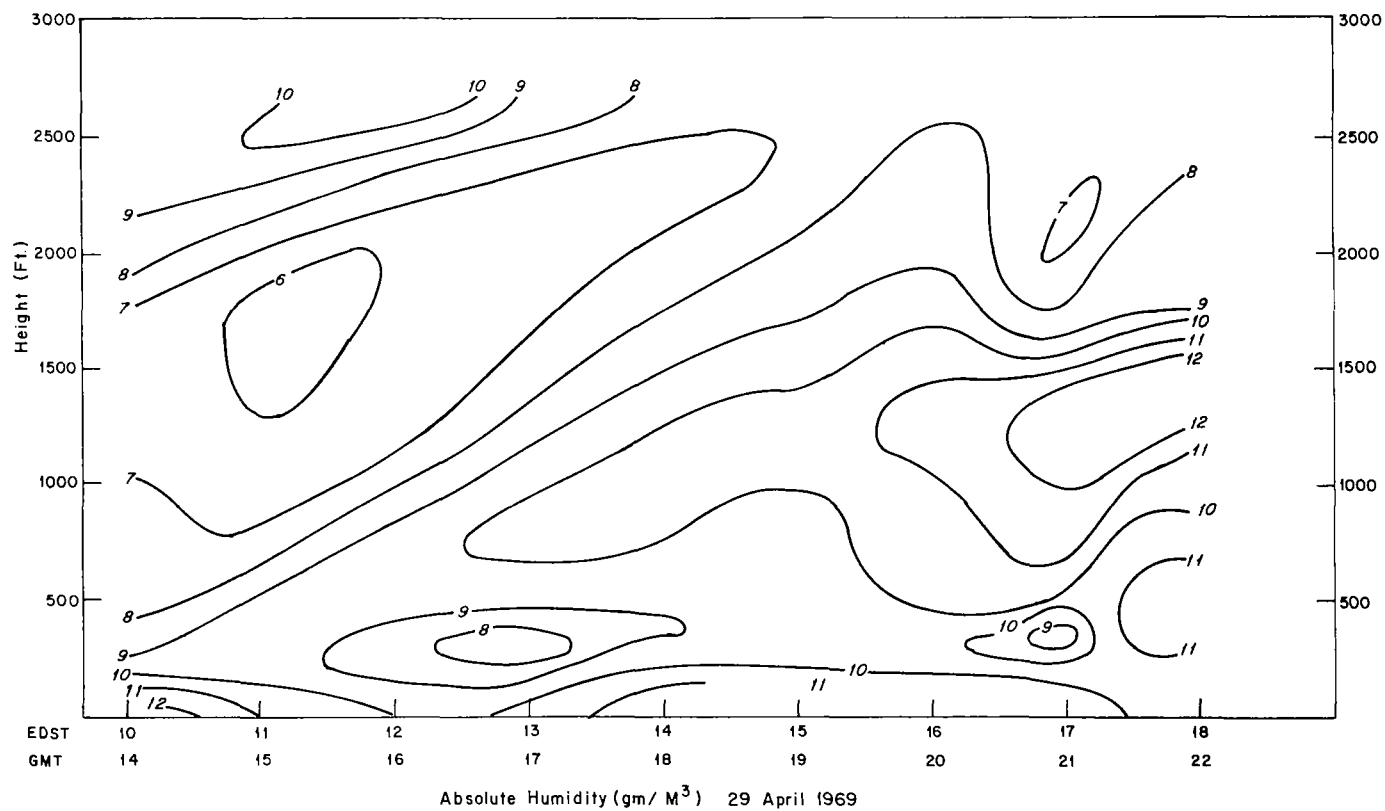


FIGURE 6. ABSOLUTE HUMIDITY VARIATION DURING AFTERNOON FLYOVER MEASUREMENTS

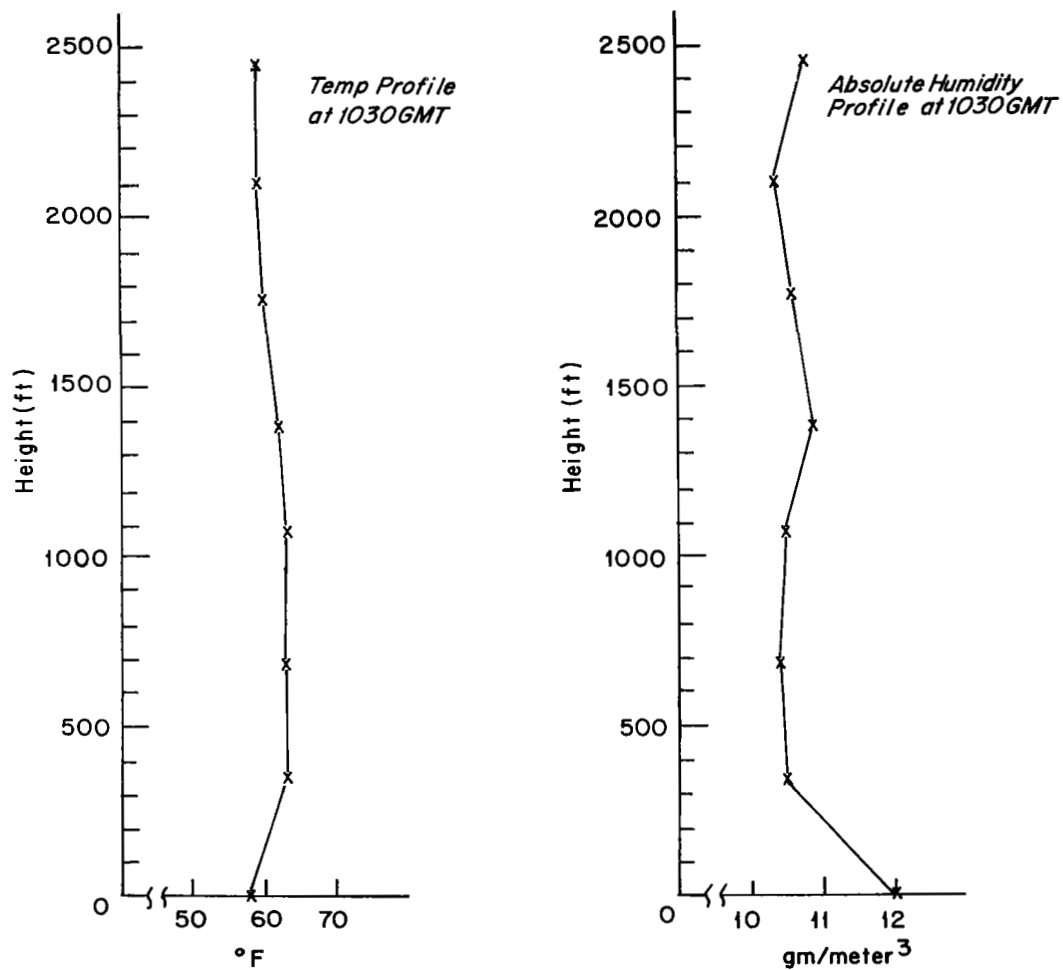


FIGURE 7. APPROXIMATE TEMPERATURE AND ABSOLUTE HUMIDITY PROFILES DURING MORNING FLYOVER MEASUREMENTS

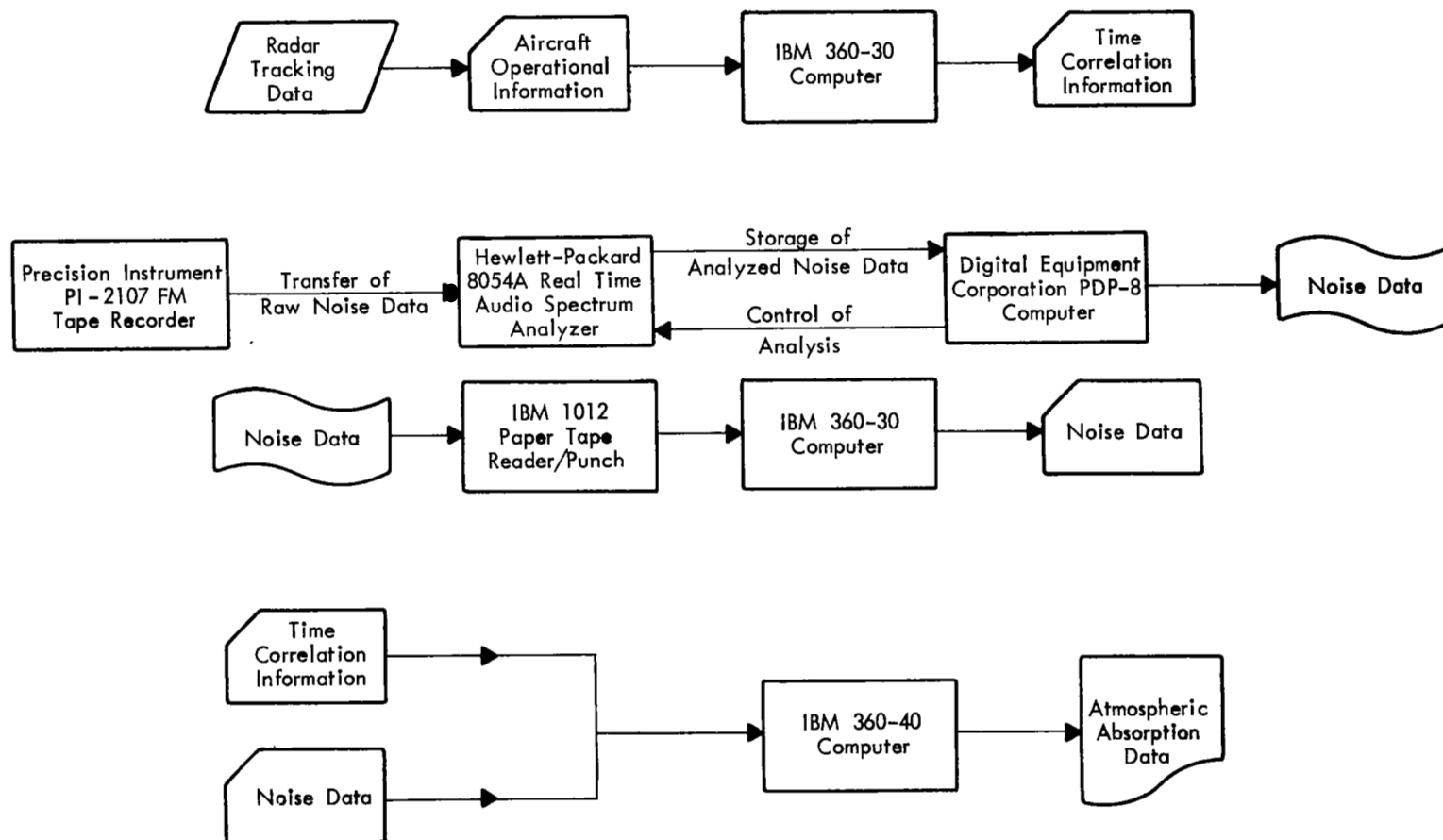


FIGURE 8. SCHEMATIC OF DATA ANALYSIS

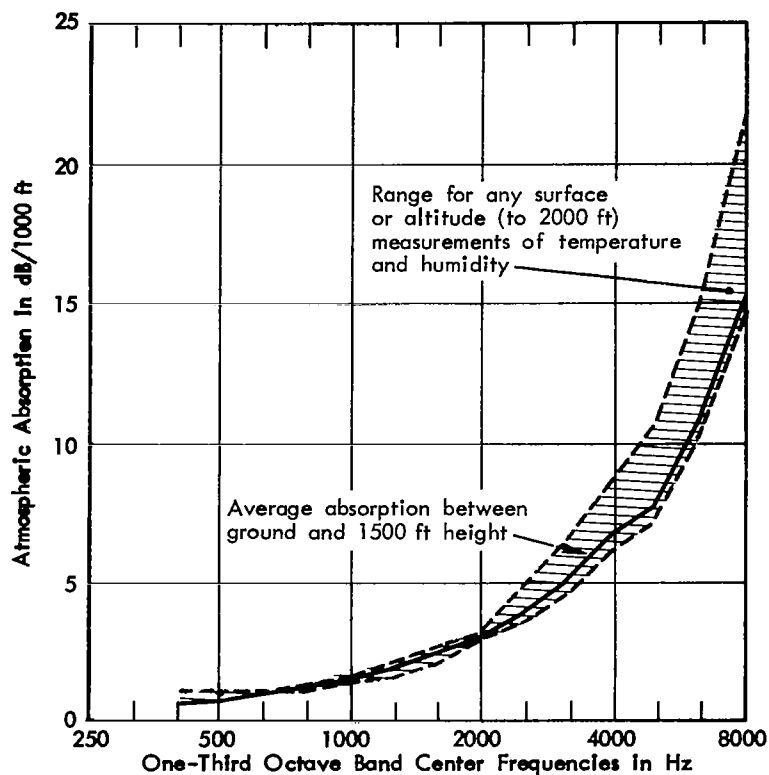


FIGURE 9. ATMOSPHERIC ABSORPTION VALUES FOR SURFACE AND ALTITUDE MEASUREMENTS OF TEMPERATURE AND HUMIDITY, CALCULATED IN ACCORDANCE WITH SAE ARP 866

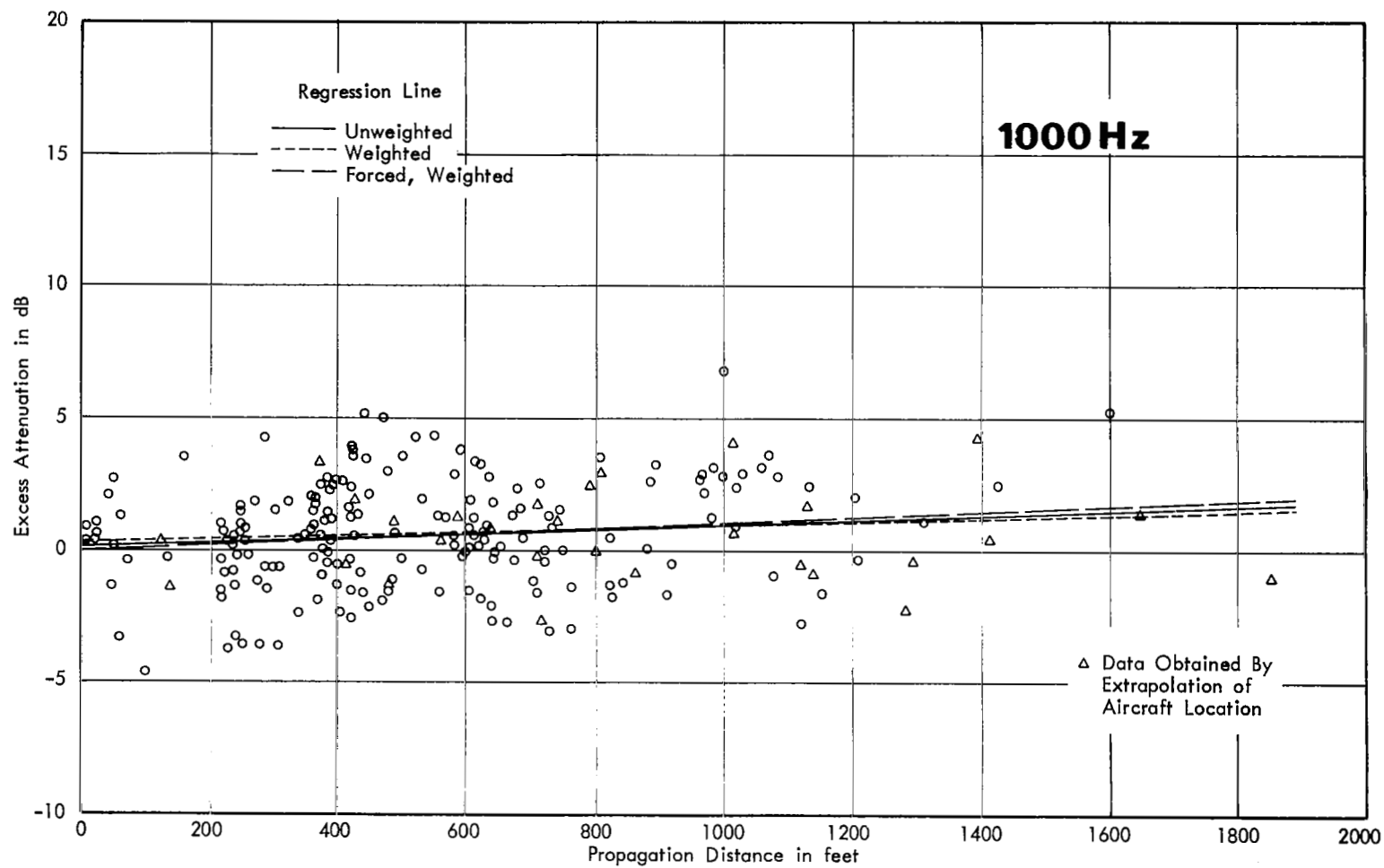


FIGURE 10. EXCESS ATTENUATION VERSUS INCREMENTAL PROPAGATION DISTANCE  
Convair 880 Flyover, 1500 ft. Altitude, Afternoon Run (Event 211) - 1000 Hz

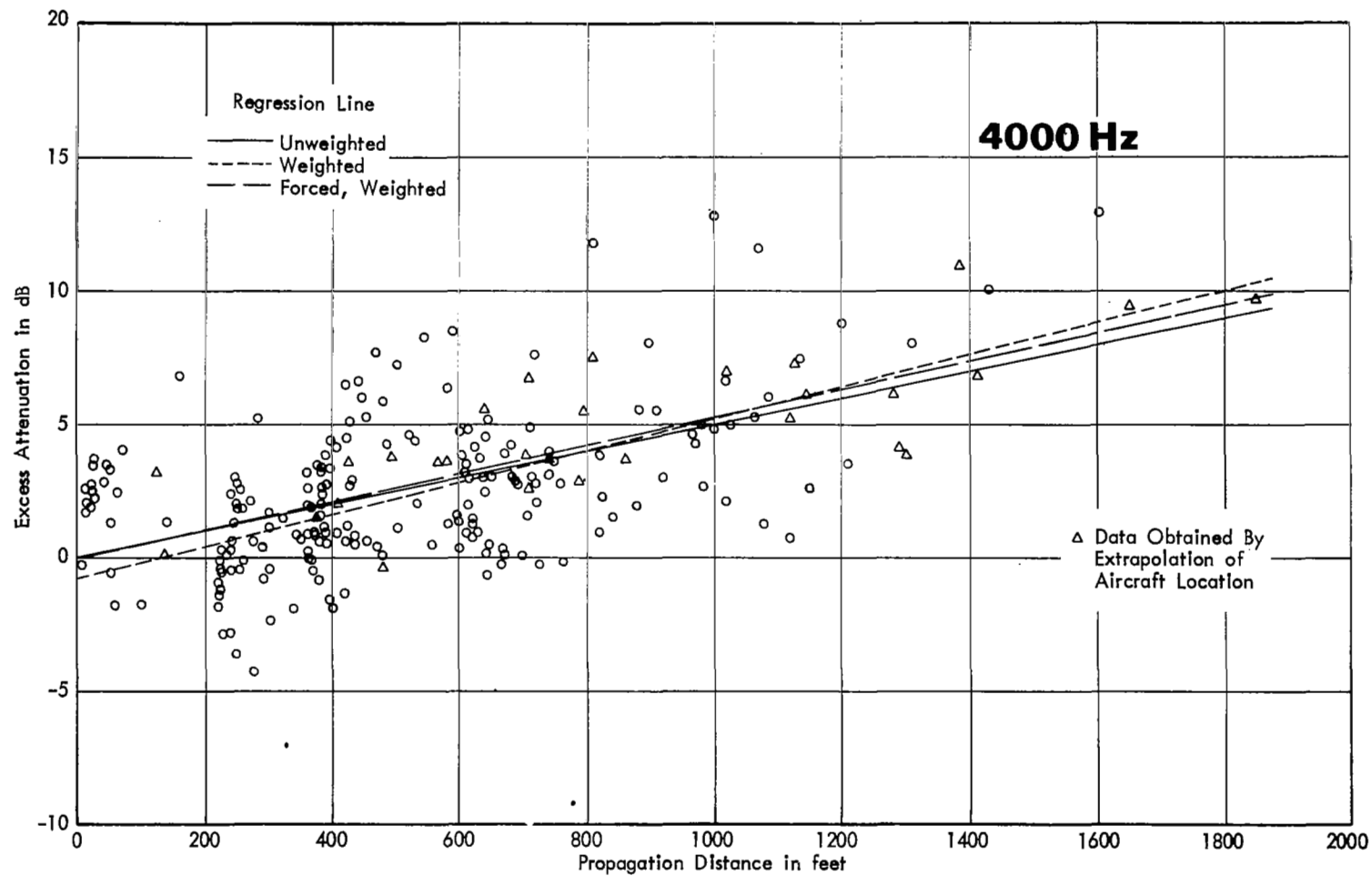


FIGURE 11. EXCESS ATTENUATION VERSUS INCREMENTAL PROPAGATION DISTANCE  
Convair 880 Flyover, 1500 ft. Altitude, Afternoon Run (Event 211)- 4000 Hz

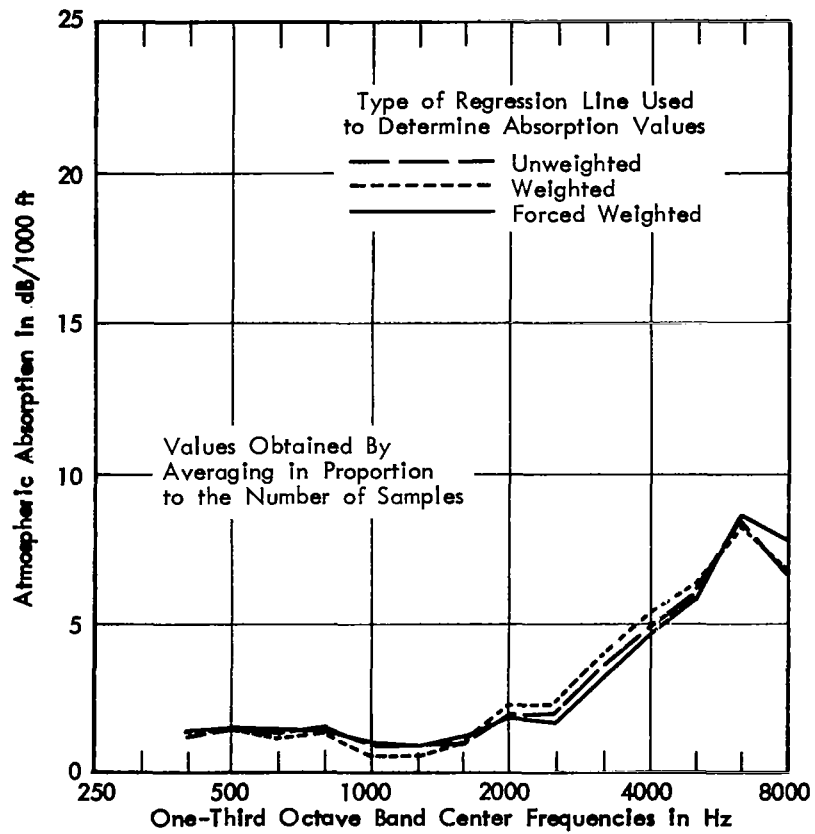


FIGURE 12. COMPARISON OF AVERAGE ABSORPTION CURVES FROM DIFFERENT TYPES OF REGRESSION LINES  
Afternoon Runs of the Convair 880

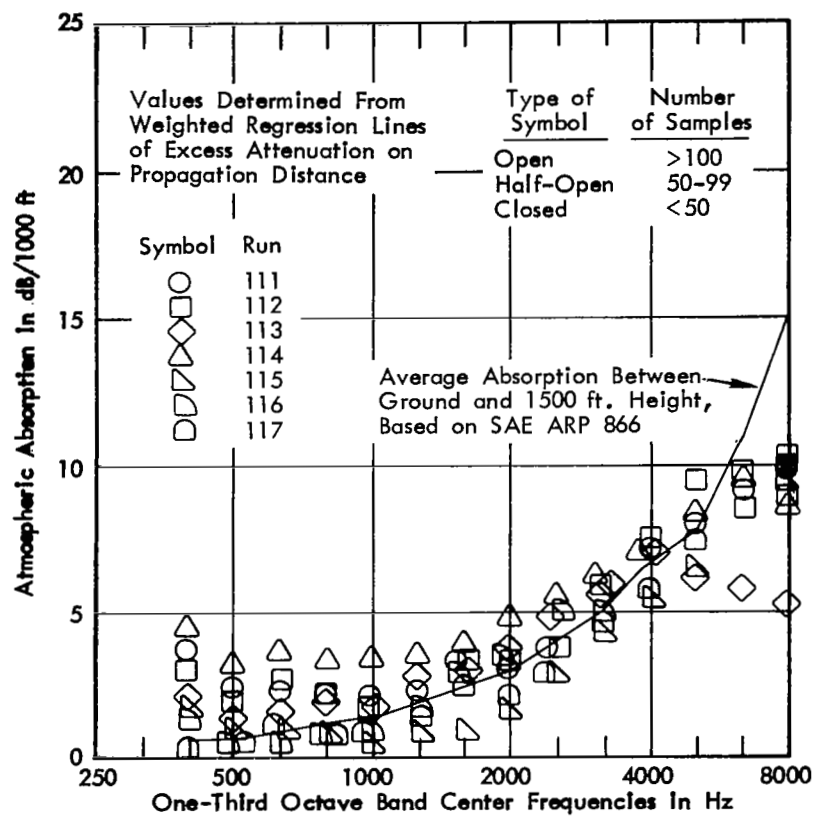


FIGURE 13. VARIATION OF ATMOSPHERIC ABSORPTION WITH FREQUENCY  
Morning Runs of the Convair 880



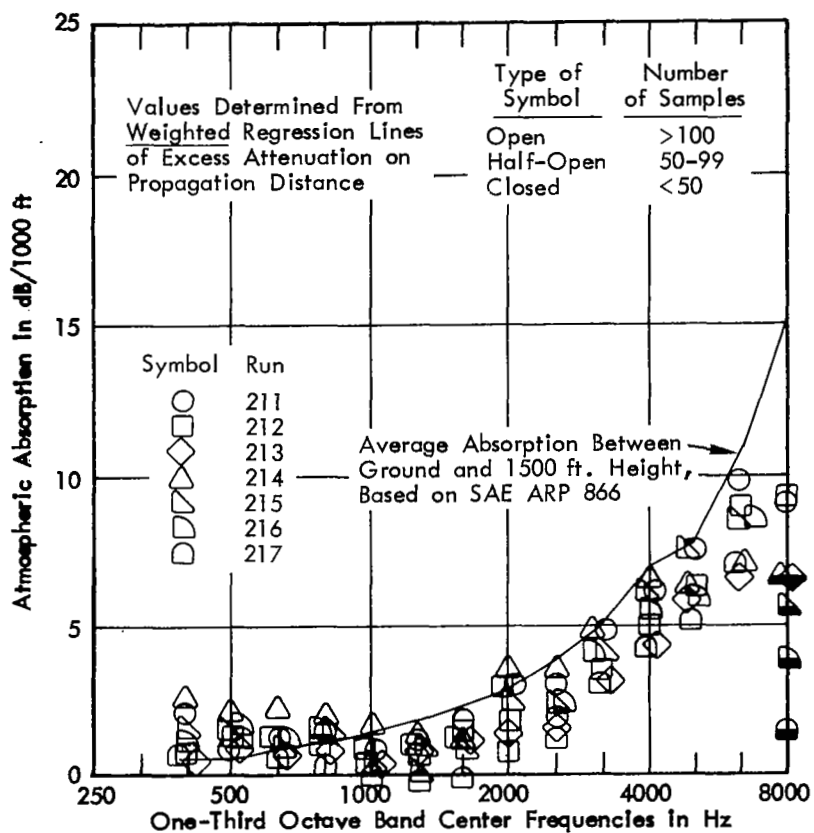


FIGURE 14. VARIATION OF ATMOSPHERIC ABSORPTION WITH FREQUENCY  
Afternoon Runs of the Convair 880

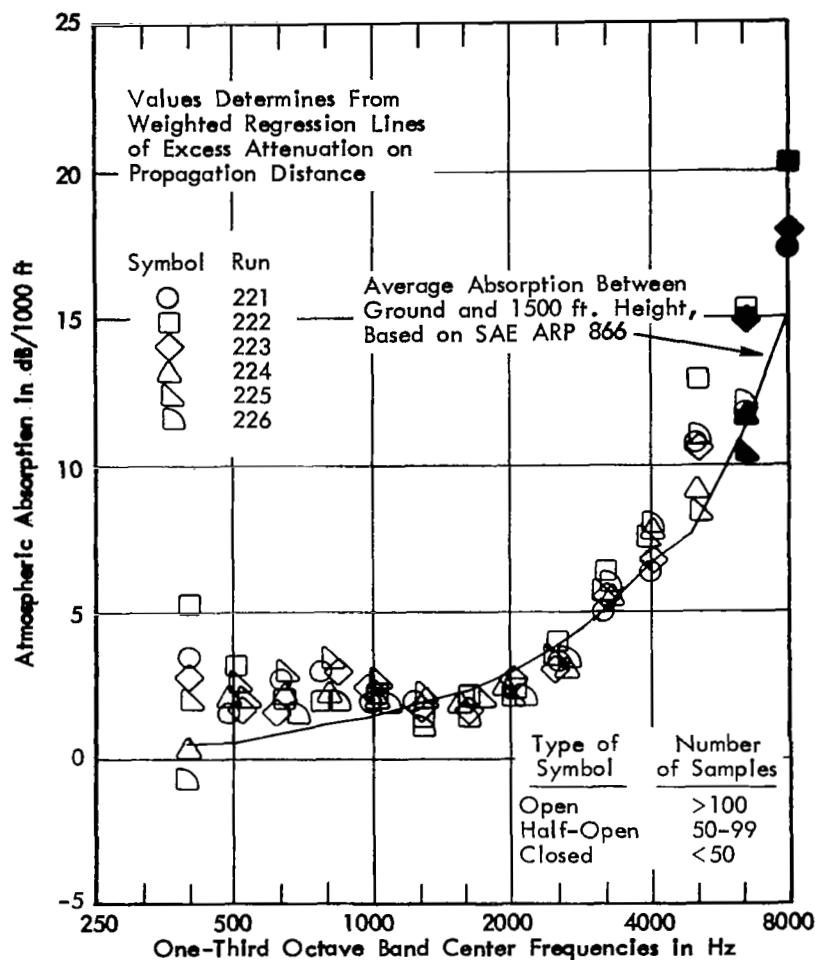


FIGURE 15. VARIATION OF ATMOSPHERIC ABSORPTION WITH FREQUENCY  
Afternoon Runs of the Lockheed 1049G

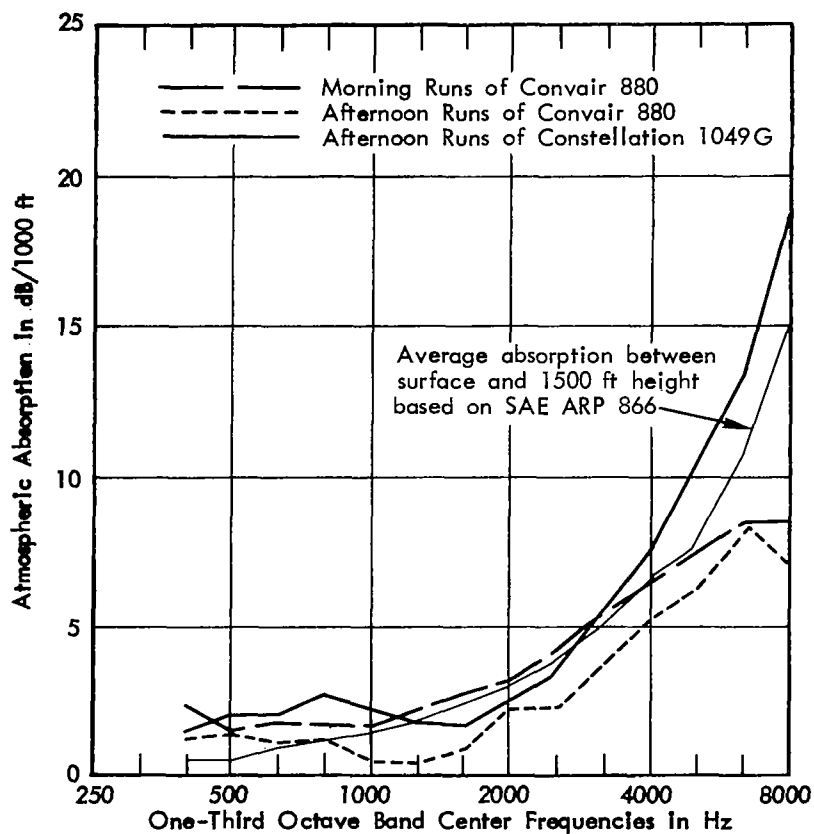


FIGURE 16. COMPARISON OF AVERAGE ATMOSPHERIC ABSORPTION CURVES  
(Extrapolated Tracking Data Included)

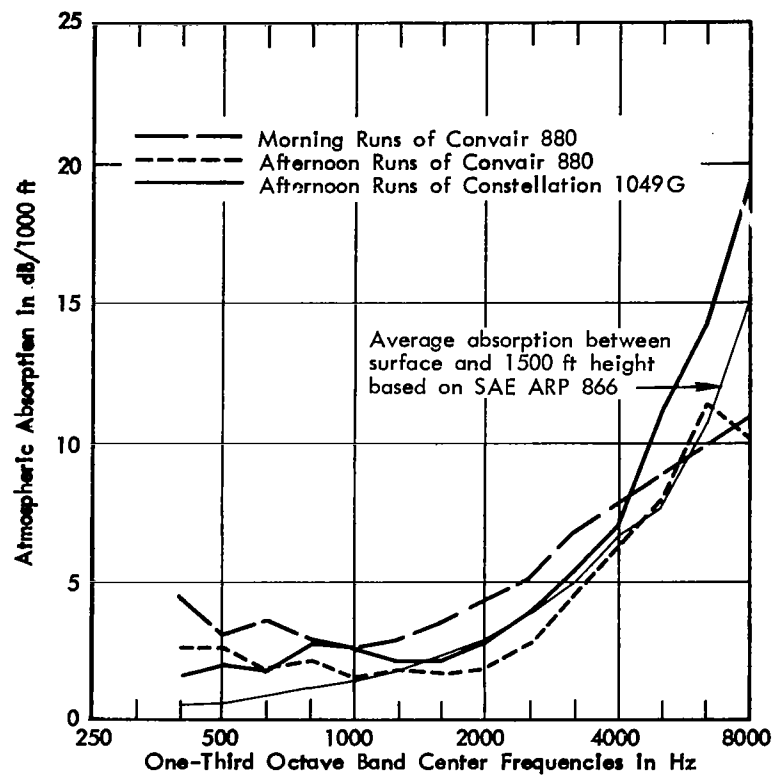


FIGURE 17. COMPARISON OF AVERAGE ATMOSPHERIC ABSORPTION CURVES  
(Extrapolated Tracking Data Removed)

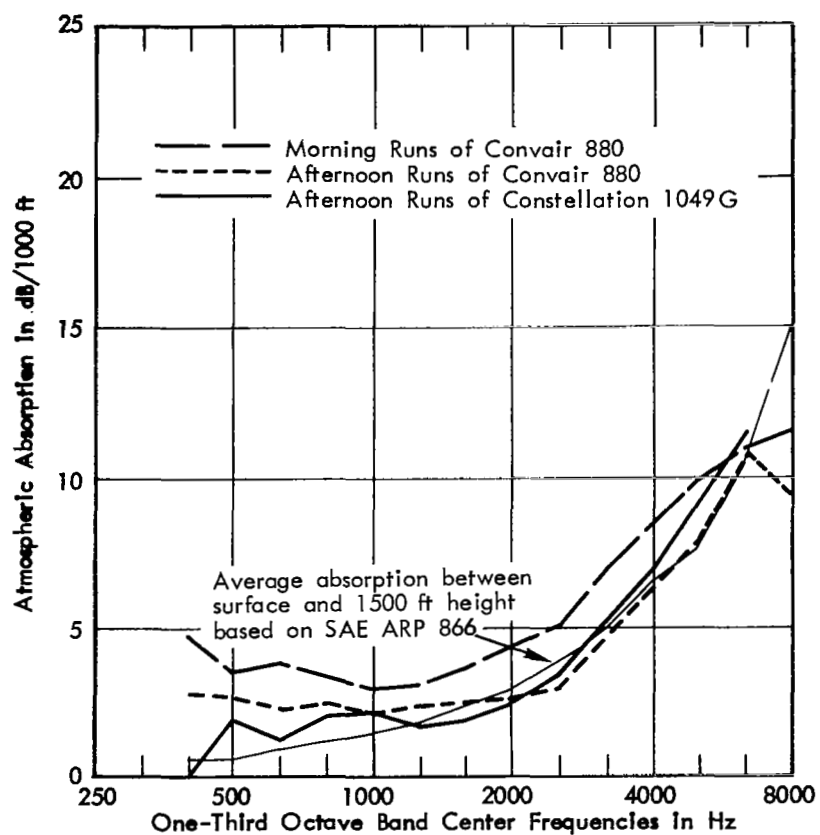


FIGURE 18. COMPARISON OF AVERAGE ATMOSPHERIC ABSORPTION CURVES FOR FLIGHTS AT 1500 FT ALTITUDE (Extrapolated Tracking Data Removed)

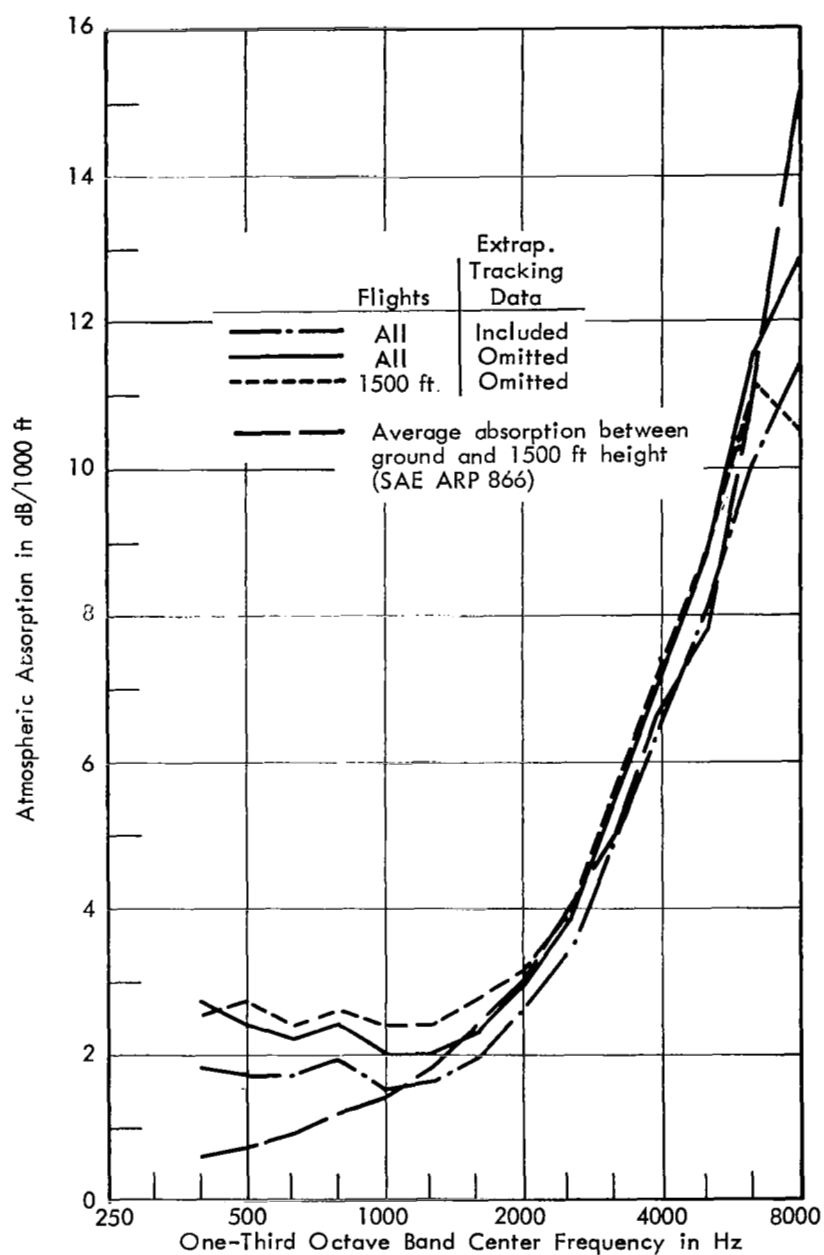


FIGURE 19. COMPARISON OF AVERAGE EXPERIMENTAL VALUES OF ATMOSPHERIC ABSORPTION WITH SAE 866 CALCULATED VALUES

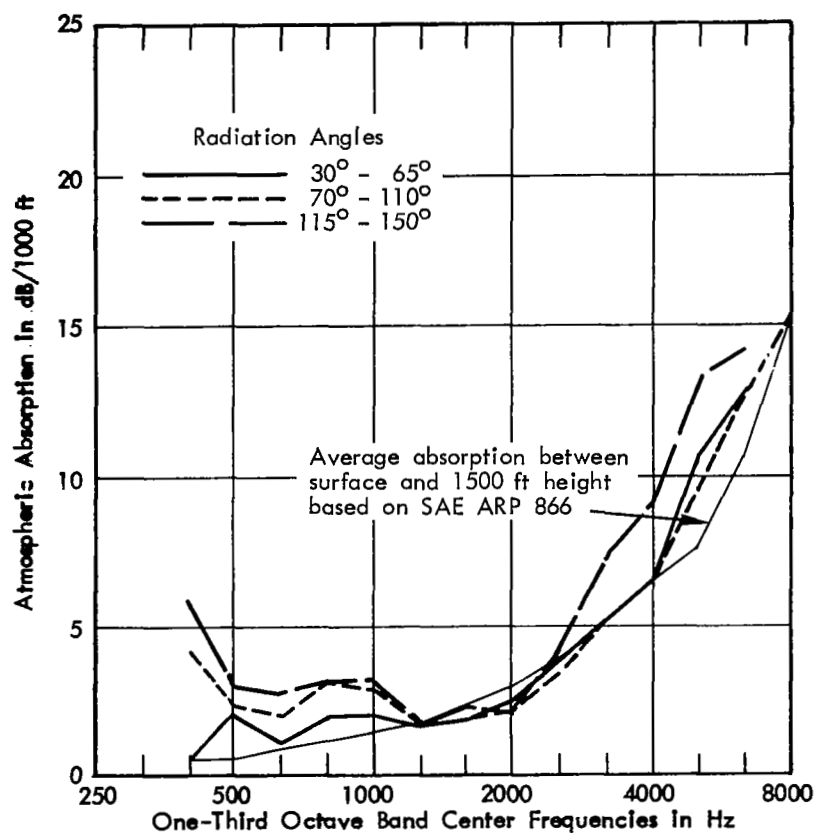


FIGURE 20. AVERAGE ATMOSPHERIC ABSORPTION CURVES FOR DIFFERENT RADIATION ANGLES - LOCKHEED 1049G (Extrapolated Tracking Data Removed)

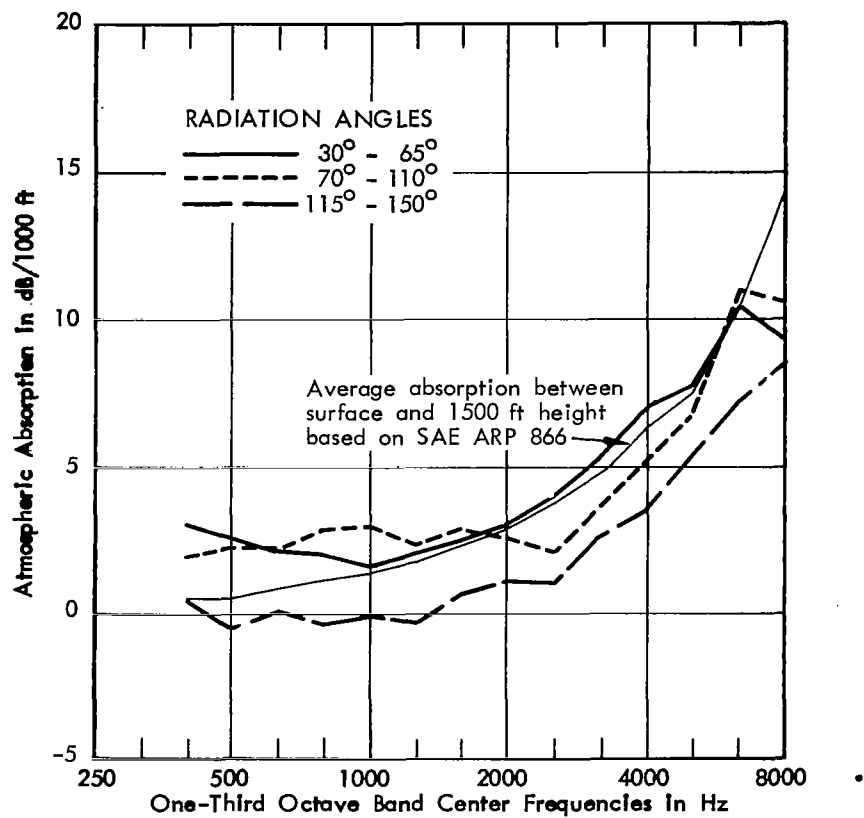


FIGURE 21. AVERAGE ATMOSPHERIC ABSORPTION CURVES FOR  
DIFFERENT RADIATION ANGLES  
CONVAIR 880 (Extrapolated Tracking Data Removed)



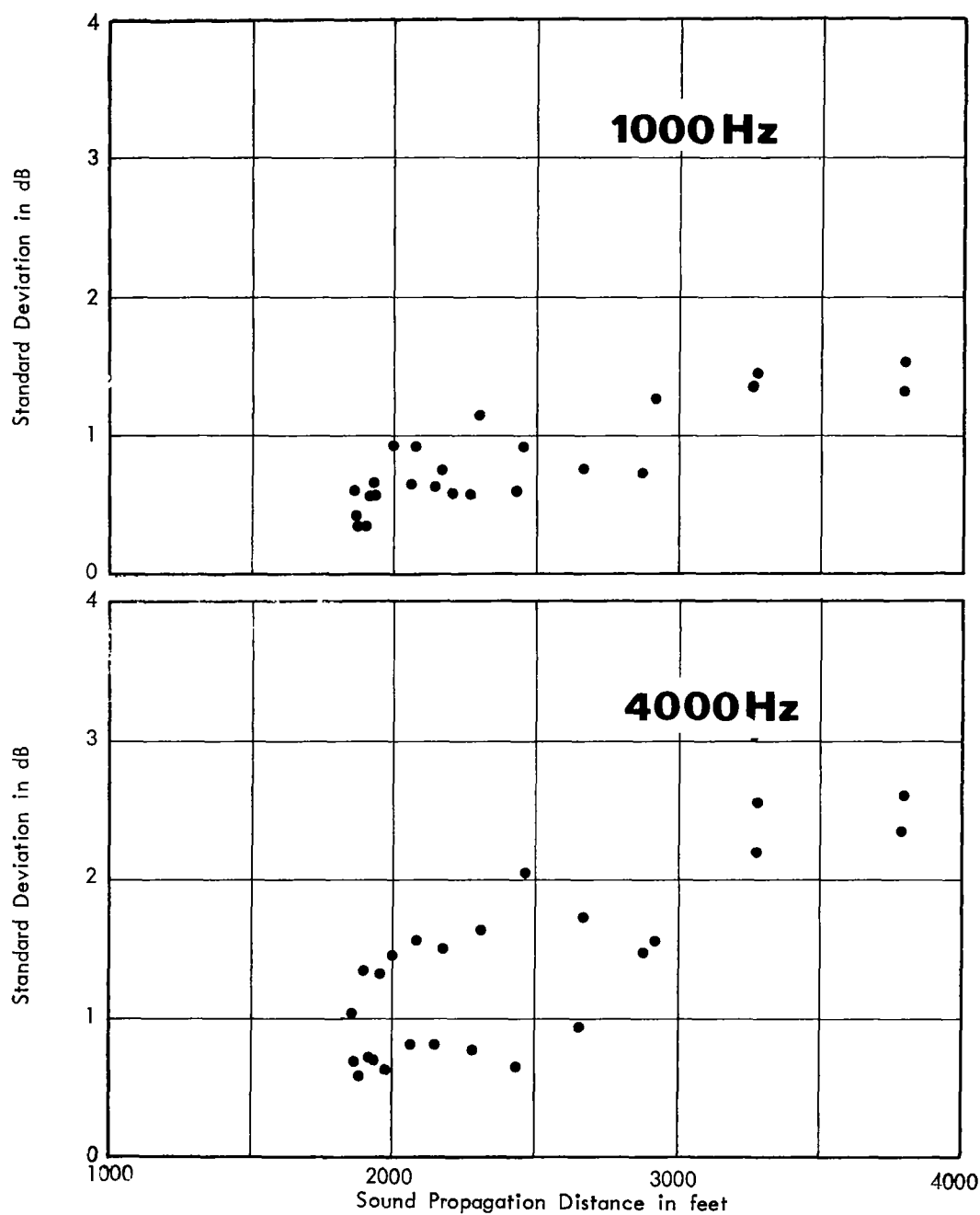


FIGURE 22. STANDARD DEVIATION FOR SEVEN REPEAT MEASUREMENTS OF ONE-THIRD OCTAVE BAND SOUND LEVELS DURING TURBOJET TRANSPORT AIRCRAFT FLYOVERS AT 2000 FT ALTITUDE (Position 2, Beneath Flight Path)

## APPENDIX A

### METEOROLOGICAL DESCRIPTIONS

Conventional surface charts for 29 April 1969 show that a frontal passage occurred over Wallops in the early morning hours prior to the 1200 GMT (0800EDST) map time. However, the surface-recorded data at Wallops only showed weak indications of such a frontal passage. At 1100 GMT, the surface wind direction turned sharply from southerly to northeasterly, then northerly. However, all through this period the surface wind speed never exceeded 3 ft/sec. The two thermograph traces both recorded temperature maxima during the night at 0600 GMT, followed by a subsequent drop of some 6° F in four hours. By this time the surface relative humidity was reported to be 100%. All through this period, the variations in surface pressure never exceeded 0.02 inches.

By 1200 GMT, surface heating effects were beginning to be reflected in the data. The temperature steadily rose to a maximum at approximately 1500 GMT. The surface winds became more turbulent with gusts reaching 16 ft/sec. These changes were accompanied by a drying-out of the surface layer. By 1700 GMT, the wind, which had been blowing from east-northeast, became decidedly easterly, suggesting the onset of the sea breeze. Subsequently, the surface temperature decreased steadily. These variations in surface parameters for the time period in question are summarized in Table II of the report.

The surface temperature and humidity recorded at the two sites did not agree at all times. The largest discrepancies occurred during the afternoon periods of maximum surface heating. The high temperature of 70° F reached at the noise measurement station was not reached at the end of the runway. At this point, a high of only 62° F was measured. Similarly,

the range of relative humidity recorded at the end of the runway, subsequent to 1500 GMT was less than that recorded at the noise measurement station for the same period. Since prior to this time, both sensors were reported approximately the same values, it appears that the differences subsequent to 1500 GMT are not due to instrument errors but reflect local differences in atmospheric conditions.

The upper air data, up to 3000 ft, are summarized in the time-sections of temperature and absolute humidity shown in Figs. 5 and 6 in the report; time profiles of wind are shown in Fig. A-1. These analyses were extended to the surface by using the mean values of the temperature and humidity recorded by the two hygrothermographs discussed previously. Because of the inadequate time continuity in the upper air data for the morning period, the time sections have been drawn only for the period subsequent to 1400 GMT. For comparison, the interpolated profiles at 1030 TMT are shown in Fig. 7 of the report. The most significant features in these analyses are: (a) The upward penetration of the surface heating effect between 1400 GMT and 1800 GMT; (b) the rapid changes to near isothermal structure in the lower layer between 1800 GMT and 1900 GMT; (c) the subsequent penetration of a "cold tongue" into the lower layers; and (d) the formation of a moist layer between 1000 ft and 1500 ft subsequent to 2000 GMT.

These variations in atmospheric structure may have important effects on the propagation. Figure A-2 for example, shows the time section profile of the speed of sound computed from the temperature profiles shown in Fig. 5. The effects of wind have not been included. The vertical variations in the speed of sound shown can not be adequately specified from the surface data alone.

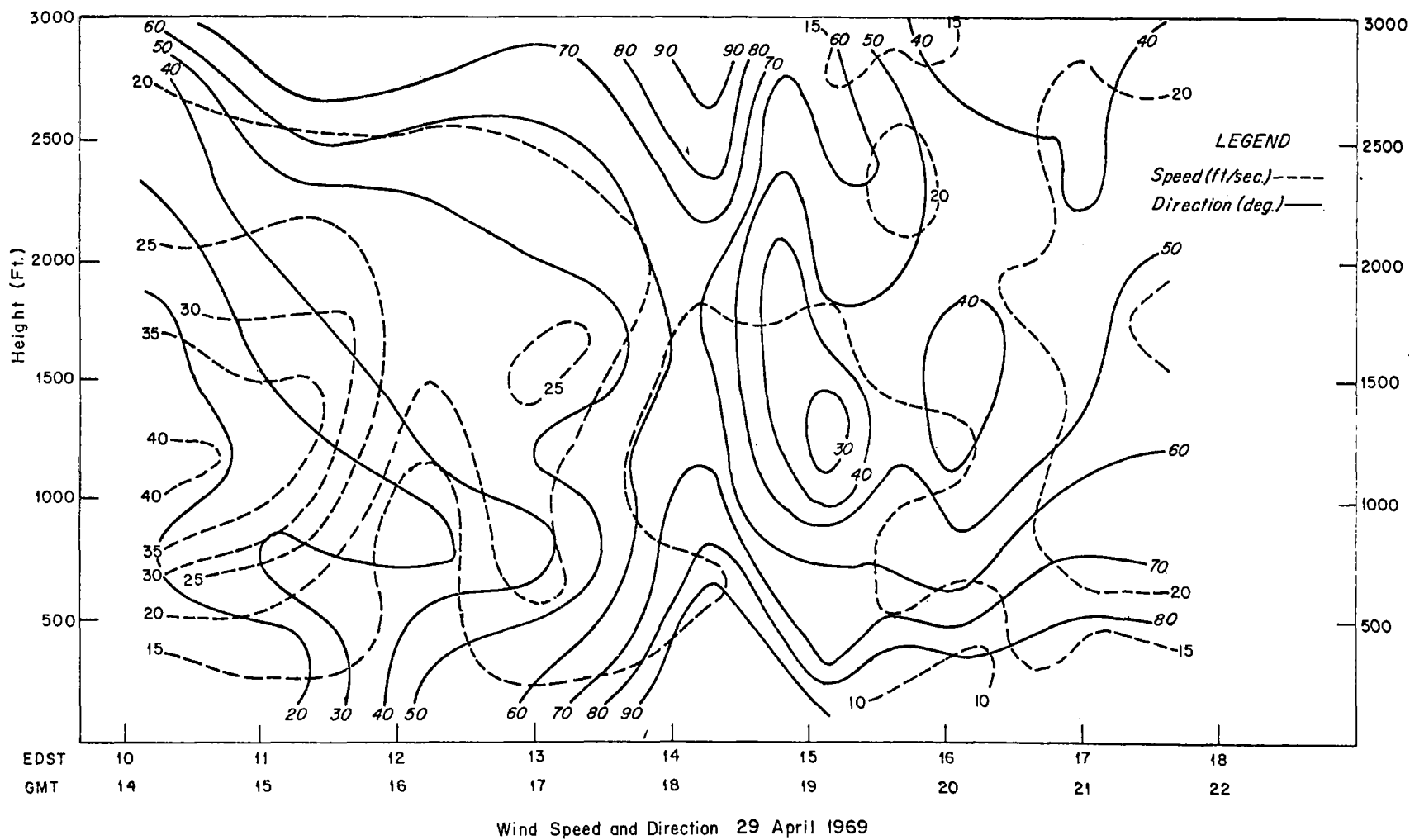


FIGURE A-1. VARIATION IN WIND SPEED AND DIRECTION DURING FLYOVER MEASUREMENTS

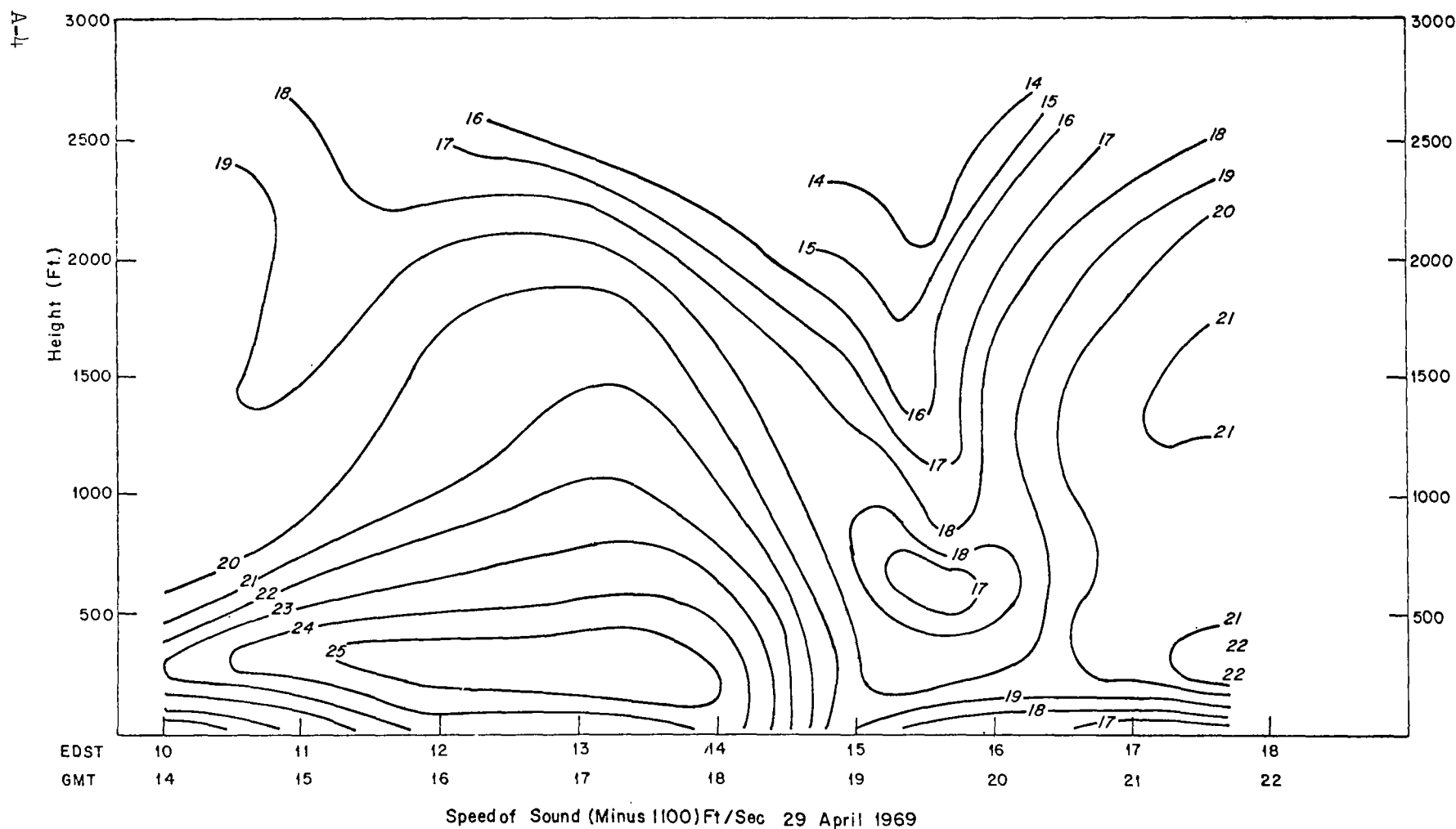


FIGURE A-2. VARIATION IN THE SPEED OF SOUND DURING FLYOVER MEASUREMENTS

## APPENDIX B

### DESCRIPTION OF COMPUTATIONS

This appendix summarizes the various calculations utilized in the data analysis. As seen in Figure B-1, the actual path of an aircraft in flight varies about a straight line path. The actual path of the flyovers in this study, as depicted on the appropriate radar traces, was approximated by straight line segments; the Cartesian coordinates of these segments, relative to the radar zero point, were obtained as a function of time from the radar traces and accompanying time marks. For each flight, this information, together with the coordinates of the ground measurement positions, was used as input to a computer program. This program calculated, by linear interpolation of the input data, the position of the aircraft at one second intervals for one minute, starting at the time for which the coordinates of the aircraft were first known.

If the time period covered by the input data was less than 60 seconds, the program extrapolated aircraft positions for the times following the known time period by assuming that the aircraft was flying directly over the flight track with the same speed as that in the latest time interval for which its actual speed was known. The assumed altitude was obtained by taking a time-weighted average of the known altitudes.

For each time increment, the angle of radiation,  $\theta_R$ , from the aircraft to each measurement position was determined according to the following equation (see Figure B-1):

$$\theta = 180^\circ - \text{arc cosine } \frac{d_1^2 + d_2^2 - d_3^2}{2d_1d_2} \quad (\text{B-1})$$

where  $\theta$  = Angle of radiation

$d_1$  = Propagation distance

$d_2$  = Distance of the aircraft along the straight line segment describing its flight path at the time under consideration

$d_3$  = Distance from measurement position to the beginning of this line segment

$d_4$  = Distance from measurement position to ground point underneath the aircraft

The radiation times ( $t_\theta$ ) corresponding to angles of radiation of  $30^\circ$  to  $150^\circ$  at  $5^\circ$  increments were determined for each measurement position by interpolation of this angle-time relationship. Then, for each of these radiation angles, the propagation distance was calculated from the coordinates of the aircraft and the measurement position. Also computed were the angle of elevation of the aircraft and the propagation time:

$$X = \text{arc tangent } \frac{h}{d_4} \quad (\text{B-2})$$

$$t_p = t_\theta + \frac{d_1}{c} \quad (\text{B-3})$$

where  $X$  = Angle of elevation

$h$  = Height of aircraft

$c$  = Average value of speed of sound

$t_p$  = Time at which the noise radiated from the aircraft at an angle is received on the ground

The next calculation step consisted of comparing the propagation distances to the different measurement positions for the same angle of radiation. For each pair of positions the difference in propagation distances was obtained, as well as the amount of inverse-square attenuation based on the ratio of the propagation distances.

For example, if  $d_{1A}$  and  $d_{1B}$  represent the propagation distances to positions A and B, respectively, and if  $d_{1A} < d_{1B}$ , then

$$d_{AB} = d_{1B} - d_{1A} \quad (B-4)$$

$$\text{and } IA_{AB} = 20 \log \frac{d_{1B}}{d_{1A}} \quad (B-5)$$

where  $d_{AB}$  is the incremental propagation distance and  $IA_{AB}$  is the inverse-square attenuation between the two positions. Incremental propagation distances and inverse-square attenuations were calculated for each position pair at each angle of radiation, except for the situation in which the angle of elevation of the aircraft from some particular position was less than or equal to  $20^\circ$ .

The input data to a second computer program were the one-third octave band noise spectra at half-second intervals received at each measurement position, and the propagation times for each radiation angle, calculated earlier. Using these times the noise levels received at each position for the various radiation angles were determined by interpolation of the half-second noise data for each frequency band.

In addition, the half-second time histories of each frequency received at each position were plotted by the computer. From these plots the noise floor was read by eye. The noise levels as a function of radiation angle were next corrected for the influence of the background noise by logarithmically subtracting the noise floor from the appropriate level. All noise levels within 3 decibels of the noise floor were eliminated from the analysis.

The adjusted levels for each radiation angle were then taken two at a time and matched with the appropriate incremental propagation distance and inverse-square attenuation values



computed previously. The excess attenuation,  $m$ , was then calculated by taking the difference in adjusted levels and removing the inverse-square attenuation. Thus, if  $L_A$  and  $L_B$  are the corrected sound pressure levels in a frequency band received at positions A and B (propagated over distances  $D_{1A}$  and  $D_{1B}$ ) respectively, then

$$m_{AB} = L_A - L_B - 1A_{AB} \quad (B-6)$$

For each radiation angle ( $30^\circ$  to  $150^\circ$  at  $5^\circ$  increments), values of  $m$  vs  $d$  were obtained in this manner for all the corrected data, in each frequency band.

Linear regression lines were fitted to the values of excess attenuation vs incremental propagation distance. The regression lines are of the form

$$m = a_0 + a_1 d \quad (B-7)$$

The values of  $a_0$  and  $a_1$  were obtained in three different ways: by standard least-squares regression analysis, by a weighted regression analysis, and by a forced-intercept weighted regression analysis.

The standard, or unweighted, regression lines were calculated from:

$$a_0 = \frac{\sum d^2 \sum m - \sum d m}{N \sum d^2 - (\sum d)^2} \quad (B-8)$$

$$a_1 = \frac{N \sum d m - \sum d \sum m}{N \sum d^2 - (\sum d)^2} \quad (B-9)$$

where  $N$  is the number of data points in the sample.

The weighted regression utilizes a weighting factor linearly proportional to the propagation distance for each data point. For this type of line, the following formulas were used:

$$a_0 = \frac{\sum d^3 \sum d m - \sum d^2 \sum d^2 m}{\sum d^3 \sum d - (\sum d^2)^2} \quad (B-10)$$

$$a_1 = \frac{\sum d \sum d^2_m - \sum d^2 \sum d_m}{\sum d^3 \sum d - (\sum d^2)^2} \quad (B-11)$$

Finally, in addition to a linear weighting factor, the forced-weighted regression line is designed to pass through the zero point of the data, i.e. zero attenuation for a propagation distance of zero. It was computed using

$$a_0 = 0 \quad (B-12)$$

$$a_1 = \frac{\sum d^2_m}{\sum d^3} \quad (B-13)$$

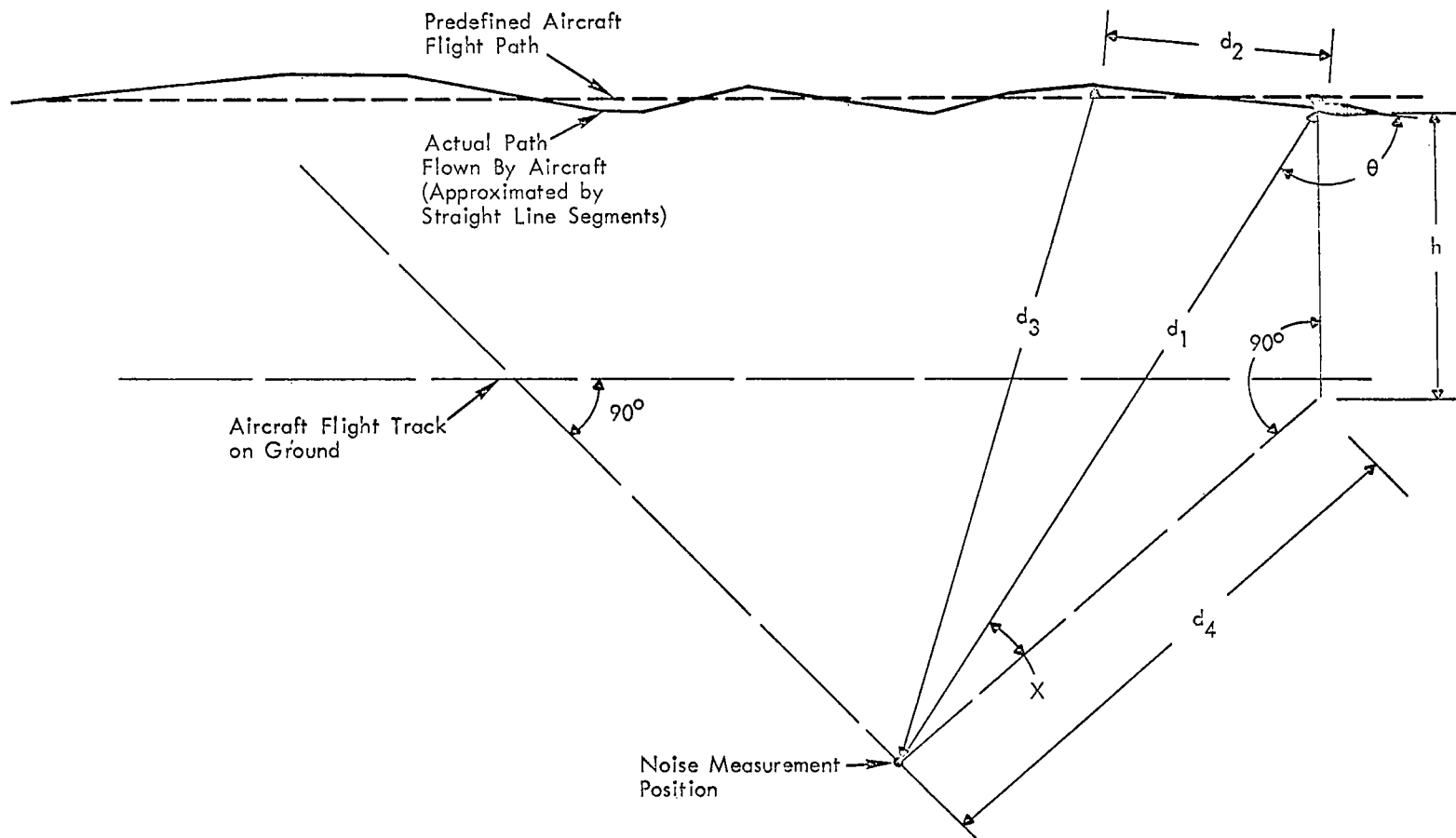


FIGURE B-1. SKETCH ILLUSTRATING PROPAGATION DISTANCE AND ANGLES DURING NOISE MEASUREMENTS OF AN AIRCRAFT FLYOVER